Updating Rainfall Intensity-Duration-Frequency Curves in Sweden Accounting for the Observed Increase in Rainfall Extremes

Sofia Eckersten

UPPSALA
UNIVERSITET

Abstract

Updating Rainfall Intensity-Duration-Frequency Curves in Sweden Accounting for the Observed Increase in Rainfall Extremes

Increased extreme precipitation has been documented in many regions around the world, including central and northern Europe. Global warming increases average temperature, which in turn enhances atmospheric water holding capacity. These changes are believed to increase the frequency and/or intensity of extreme precipitation events. In determining the design storm, or a worst probable storm, for infrastructure design and failure risk assessment, experts commonly assume that statistics of extreme precipitation do not change significantly over time. This so-called notion of stationarity assumes that the statistics of future extreme precipitation events will be similar to those of historical observations. This study investigates the consequences of using a stationary assumption as well as the alternative: a non-stationary framework that considers temporal changes in statistics of extremes. Here we evaluate stationary and non-stationary return levels for 10-year to 50-year extreme precipitation events for different durations (1-day, 2-day, ..., 7-day precipitation events), based on the observed daily precipitation from Sweden. Non-stationary frequency analysis is only considered for stations with statistically significant trends over the past 50 years at 95% confidence (i.e., 15 to 39 % out of 139 stations, depending on duration, 1-day, 2-day, ..., 7-day). We estimate non-stationary return levels using the General Extreme Value distribution with time-dependent parameters, inferred using a Bayesian approach. The estimated return levels are then compared in terms of duration, recurrence interval and location. The results indicate that a stationary assumption might, when a significant trend exists, underestimate extreme precipitation return levels by up to 40 % in Sweden. This report highlights the importance of considering better methods for estimating the recurrence interval of extreme events in a changing climate. This is particularly important for infrastructure design and risk reduction.

Keywords: IDF curves, climate change, non-stationarity, stationary, Sweden, return level, return period, NEVA, GEV, extreme value analysis

Referat

Uppdatering av Intensitets-Varaktighetskurvor i Sverige med hänsyn till observerade ökande trender av extrem nederbörd

Ökad extrem nederbörd har dokumenterats globalt, däribland centrala och norra Europa. Den globala uppvärmningen medför en förhöjd medeltemperatur vilket i sin tur ökar avdunstning av vatten från ytor samt atmosfärens förmåga att hålla vatten. Dessa förändringar tros kunna öka och intensifiera nederbörd. Vid bestämning av dimensionerande nederbördsintensiteter för byggnationsprojekt antas idag att frekvensen och storleken av extrem nederbörd inte kommer att förändras i framtiden (stationäritet), vilket i praktiken innebär ingen förändring i klimatet. Den här studien syftar till att undersöka effekten av en icke-stationärt antagande vid skattning av dimensionerande nederbördsintensitet. Icke-stationära och stationära nerderbördsintensiteter för återkomsttider mellan 10 och 100 år bestämdes utifrån daglig och flerdaglig svensk nederbördsdata. Nederbördintensiteterna bestämdes med extremvärdesanalys i mjukvaran NEVA, där den generella extremvärdesfördelningen anpassades till årlig maximum nederbörd på platser i Sverige som påvisade en ökande trend under de senaste 50 åren (15% till 39 % utav 139 stationer, beroende på varaktighet). De dimensionerande nederbördsintensiteterna jämfördes sedan med avseende på varaktighet, återkomsttid och plats. Resultaten indikerade på att ett stationärt antagande riskerar att underskatta dimensionerande nederbördsintensiteter för en viss återkomsttid med upp till 40 %. Detta indikerar att antagandet om icke-stationäritet har större betydelse för olika platser i Sverige, vilket skulle kunna ge viktig information vid bestämning av dimensionerande regnintensiteter.

Nyckelord: Intenstitets-varaktighetskurvor, Klimatförändring, Icke-stationäritet, stationäritet, Sverige, flerdaglig nederbörd, dimensionerande nederbördsintensitet, återkomsttid, NEVA, GEV, extremvärdesanalys

Preface

This Master's thesis is the final part of the M.Sc. in Environmental and Water Engineering at Uppsala University and is an independent project corresponding to 30 ETCS. The project was started and ended in Stockholm, but was performed mainly at the University of Irvine (UCI), in California. I spent four months in Irvine working as a visiting scholar in the research group of Professor Amir AghaKouchak. My time there was more challenging and instructive then I expected. Apart from the opportunity of writing my thesis I have increased my understanding of a different working practice, other fields of research, people and cultures, and myself.

Many people have contributed to making this work possible. First of all I wish to thank Professor Amir AghaKouchak and his extraordinary research group at UCI, of whom I worked closest to Elisa Ragno, Alireza Farahmand, Hamed Moftakhari, Felicia Chiang, Charlotte Love, Omid Mazdiyasni, Hassan Anjileli, Samaneh Ashraf, Juan Rivadeneira and Yasir Ak. Their knowledge, support and engagement made it possible for me to undertake this project. A special thank you to Linyin Cheng, with co-authers, for doing the excellent work with developing NEVA software package, giving me the opportunity to use it in my work. I also wish to send my thanks to Professor Giuliano Di Baldassarre at Uppsala University, my academic supervisor who contributed with enlightening ideas along the way. Thank you also Dr Kaveh Madani at the Imperial College in London, Professor Hans Hanson at LTH (Lund university) and Professor Carola Wingren at the Swedish University of Agricultural Science; the chain of people meditating the contact with Professor Amir AghaKouchak.

Friends made in Irvine and dear friends in Sweden, the biggest thank you for encouraging words, inspiration and laughs throughout this project. Finally, I wish to thank my family for always giving me the best of support in everything I undertake me.

Stockholm, Sweden, March 2016

Sofia Eckersten

Populärvetenskaplig sammanfattning

Uppdatering av Intensitets-Varaktighetskurvor i Sverige med hänsyn till observerade ökande trender av extrem nederbörd

Sofia Eckersten

Jordens medeltemperatur har ökat under det senaste århundradet till följd av klimatförändringar. Den ökande medeltemperaturen har inneburit att mängden vatten som avdunstar från ytor samt atmosfärens förmåga att hålla vatten har förändrats. Följaktligen har mängden vatten och vattenånga i atmosfären som finns tillgängligt för nederbörd tilltagit och därmed har också risken för intensivare regn ökat. På en global skala har en tilltagande trend i extrem nederbörd observerats och samma sak verkar gälla i centrala och norra Europa inklusive Sverige. Stora regnmängder under en kort tidsperiod, så väl som måttliga regnmängder under en längre tidsperiod, förhöjer risken för höga flöden och översvämningar i naturliga och urbana miljöer. Byggnadsverk dimensioneras ofta efter den maximala nederbörd som sannolikt kommer att falla under en viss tidsperiod över området där det ska byggas, kallad dimensionerande nederbördsintensitet. Exempelvis, en byggnad som förväntas stå i minst 50 år dimensioneras för att kunna motstå den högsta sannolika nederbördshändelsen inom en 50-års period (50-års regn). På så vis kan skador på infrastruktur till följd av stor och intensiv nederbörd förebyggas. Uppskattningen av dimensionerande nederbördsintensiteter med de metoder som används idag, antar att klimatet kommer att förbli detsamma i framtiden som det har varit under de senaste decenierna. Detta antagande strider mot den allmänna uppfattningen att nederbörden tilltar i vissa områden, dvs att klimatet anses icke-stationärt. Hur stor betydelse har antagandet om stationärtitet alternativt icke-stationäritet för skattningen av den "dimensionerande nederbördsintensiteten"; hur mycket underskattas den?

Sverige karaktäriseras av ett milt klimat i jämförelse med andra områden som ligger på samma breddgrad. Detta beror på närheten till Atlanten och de dominerande vindriktningarna. Västliga vindar tar med sig varm och fuktig luft utifrån havet vilket ger nederbörd över Sverige året runt. Under de senaste årtiondena har både intensivare nederörd samt att nederbördshändelserna pågår under en längre tid noterats. Dessa händelser har dessutom associerats med översvämningar, bland annat i mellersta Sverige. Frågan som har ställts i den här studien är därför ifall den årliga maximala nederbörden för perioder från en dag till en vecka har ökat över tid. Har antalet stora nederbördshändelser ökat? Hur beror den "dimensionerande nederbördsintensitetenpå ifall

icke-stationäritet antas eller inte?

För att undersöka ifall den årliga maximala dygnsnederbörden för olika varaktigheter hade ökat för en specifik plats under de senaste 50 åren gjordes ett trend test, det såkallade Mann-Kendall (MK) trend test, på den högst uppmätta dygnsnederbörden för varje påföljande hydrologiskt år (1 oktober - 31 september). Från dataserier med dagliga nederbördsdata uppmätt vid 139 olika väderstationer runt om i Sverige identifierades områden med positiva trender (20 områden). På motsvarande sätt identifierades stationer med positiva trender för längre varaktighet (2 dagar, 3 dagar...7 dagar). Totalt 12 stationer identifierades med positiva trender för alla varaktigheter upp till en vecka. Det undersöktes ocks ifall det fanns en förändring i fördelningen av den årliga maximala nederbörden mellan den första och andra halvan av 50-års perioden. Detta gjordes med Kolmogorov-Smirnov test som antydde att årliga maximala nederbörden har ökat under de senaste 25 åren. För de 20 stationer som visade på en ökande trend i dygnsnederbörd samt för de 12 stationer med en trend för varaktigheter upp till en vecka, bestämdes sedan de dimensionerande nederbördsintensiteterna (för olika varaktigheter). Detta gjordes genom att analysera sannolikheten att extrema värden på nederbörden uppkommer vid varje station, s.k. extremvärdesanalys, med hjälp av mjukvarupaketet NEVA. Två olika tillvägagångssätt användes; ett med antagandet om stationäritet och ett med antagandet om icke-stationäritet. Antagandet om icke-stationäritet antar att nederbörden förväntas öka linjärt med tiden. De dimensionerande nederbördsintensiteterna för de olika stationerna jämfördes sedan med avseende på plats, varaktighet och återkomsttid. Slutligen utvecklades också intesitets-varaktighetskurvor för antagandet om icke-stationära respektive stationära förhållanden.

Trend analysen resulterade i att vid ungefär 15 % (20 stycken) av de undersökta stationerna hade den dagliga årliga maximala nederbörden ökat. Fler stationer visade på en ökande trend för längre varaktighet, maximalt 28 % (39 stycken) för 3 dagars nederbörd. Endast 12 stationer vidhöll ökande nederbördstrender för samtliga varaktigheter. Resultaten från extremvärdesanalysen indikerade att antagandet om stationäritet skattar lägre värden på de dimensionerande nederbördsintensiteterna för en viss återkomsttid än vad antagandet om icke-stationäritet gör. Skillnaden mellan de dimensionerande regnintensiteterna varierade mellan olika platser, och var som störst i Rossared, Småland, där det skilde ungefär 25 mm/dag vilket motsvarade en relativ skillnad på 50 %. Den absoluta skillnaden minskade generellt med ökande varaktighet, vilket antydde att antagandet om icke-stationäritet har större betydelse för kortare varagtigheter (dygnsvärden).

Antagandet om icke-statinäritet vid bestämningen av intesitets-varaktighetskurvor är ett steg mot att klimatanpassa ett relativt enkelt dimesioneringsverktyg vid byggnationer. Ifall information om hur nederbörd påverkas av andra klimatvariabler n nederbrden sjlvt också beaktas, så skulle det kunna innebära mer tillförlitlig information om framtida extrem nederbörd.

Glossary

Precipitation: Condensed atmospheric water vapour falling down on earth, including snow, rain, hail etc.

Climate Change: Changes in the statistical distribution of weather patterns caused by biotic processes, variations in solar radiation, volcanic eruption, certain human activities etc.

Exceedance probability: The probability that precipitation exceeds a certain threshold

Return level: The highest expected precipitation intensity for a particular recurrence interval

Return period: The recurrence interval associated with a particular precipitation event (return level)

Design Storm: Virtual storm providing information about the expected rain intensity for a given duration and probability of occurrence

Probable maximum precipitation (PMP): The greatest accumulation of precipitation for a given duration meteorologically possible for an area

Column Water Vapour: The depth of water in a column in the atmosphere

Water year: 12 month period beginning 1 October and continuing through September 30

Null hypothesis: Refers to a general statement or default position that there is no relationship between two variables

NEVA: Non-stationary extreme value analysis software package

Prior probability distribution: Probability distribution that express beliefs about a quantity before evidence is taken into account

Posterior probability distribution: The probability distribution of an outcome given another outcome

Contents

Chapter 1

Introduction

Human activity changes the atmosphere's composition by increasing greenhouse gases (GHG)[45, 61]. These changes have subsequently increased global temperatures, surface evaporation and atmospheric water holding capacity [64, 65]. As a result, climate change may increase the amount of water available for precipitation in the atmosphere as well as increase the probable maximum precipitation (PMP) or expected extreme precipitation [4, 33]. Those changes in turn would affect society by increasing the risk of climatic extremes [13, 25] that can cause floods and damage to infrastructure. On a global basis, trends of increasing precipitation extremes have been observed [12, 45, 67]. In northern and central Europe several studies also indicate increasing trends in extreme events, e.g. in Sweden, Denmark, Czech Republic, Germany and Poland, Belgium as well as UK [3, 19, 35, 38, 48, 52]. Locations that are seeing an increase in total annual precipitation also tend to see increasing extreme events [39, 60, 57]. However, Europe's total annual precipitation also has negative trends, indicating that extreme precipitation is both intensified and de-intensified [3, 11, 16, 34, 42, 46, 49, 50, 66]. Trends are highly dependent on location, season and duration analyzed, which studies also note. Research on precipitation in southern Sweden shows that total annual precipitation has increased at some locations and that more extreme precipitation events are lasting for multiple days. These prolonged events have been mentioned in the context of flooding in southern Sweden (descriptions of flooding events are given at SMHI.se/kunskapsbanken) [3].

Hydraulic and hydrological engineers use intensity duration frequency(IDF) curves to design infrastructure that can deal with extreme precipitation and flooding [14, 15, 41, 40, 59, 63, 68]. IDF-curves can be developed with frequency analysis at sites where historical precipitation data is available. They are designed to capture the intensity and frequency of precipitation, i.e. the expected rain intensity (return level, q_p) for a given duration and the probability of occurrence (return period, T). The design storm incorporates rain intensity estimated from IDF-curves, obtained by fitting a suitable theoretical probability distribution function to the observed data [6]. The IDF-curves applied today are derived assuming that extreme events' occurrence probability does not change significantly over time [14, 29]. However, studies show that extreme events have changed over time, an observation referred to as non-stationary conditions [1, 19, 29].

Box 1: What about precipitation?

The global water cycle encompasses the balance of water on, above and below the surface of the Earth. As the mass of water remains constant, the partitioning between the major reservoirs of ice, fresh water, saline water and atmospheric water varies depending on climatic variables. The sun's radiation heats the ocean and land surfaces, thereby evaporating water into the atmosphere. Upward air movement comes from rising air over mountains, warm and cold fronts, and convection created by local heating of the surface and surrounding weather systems. The air moves around in the atmosphere, condenses to form clouds and falls back onto the surface as precipitation. The water infiltrates or runs off the landscape and ends up in the ocean, thereby completing the water cycle.[64]

Precipitation varies with time and changes in amount, intensity, frequency and type. Snow forms below freezing point, but also has variability: At low temperatures such as $-10°C$ it is dry and light whereas closer to $0°C$, larger snowflakes can form, resulting in heavier snowfalls. Snow remains on the ground during low temperatures before it runs off. At temperatures above freezing point, light precipitation can form from condensed total column water vapor (TCWV) or evaporation in the precipitation area. Moderate and heavy precipitation forms from moisture convergence over regions that are 10 to 25 times larger than those needed for light precipitation. Light to moderate precipitation soaks into the soil, providing water to plants when it falls as rain, whereas heavy rain and rapid snowmelt may cause local flooding. [64]

A strong relationship between total column water vapor and sea surface temperatures (SST) has been observed and can be described by the Clausius Clapeyron (C-C) relationship. This relationship expresses the water-holding capacity of the atmosphere as a function of temperature, typically 7% per $1°C$. The highest TCWV is found over the tropical Pacific Warm Pool and occuspies the highest large-scale values of SST. High TCWV is also observed in the Northern Hemisphere during the summers, as a consequence of higher surface temperatures. The effect of SST on TCWV is generally more substantial over seas, mainly because of unlimited supply of water. Precipitation is strongly correlated with TCWV, especially in the tropics and subtropics, indicating that precipitation also can be related to SST values. Changes in SST are also associated with SST gradients and subsequently, precipitation. Surface pressure gradients and winds also have a strong influence on precipitation. Therefore, large amounts of precipitation can be observed along the mid-latitude storm tracks, although TCWV reduces with higher latitudes (decrease in SST), [64, 65]

Atmospheric circulation patterns affect precipitation regionally and locally. In the Northern Hemisphere, fluctuations in atmospheric pressure differences at sea level between the Icelandic low and the Azores high controls the strength and direction of westerly winds as well as storm tracks across the north Atlantic. The westerly winds bring moist air into Europe affecting the climate there. Weak westerlies, i.e. those with small pressure differentials, result in warm summers and cold winters in Sweden. Strong westerlies produce cold summers, mild winters and more frequent precipitation. This phenomena is called the North Atlantic Oscillation (NAO) and has been observed to intensify the precipitation in Europe periodically. [5, 20, 55]

A simple approach to address climate-change-related alteration in extreme precipitation when developing IDF-curves is to multiply the estimated design storm with a climate factor derived from future climate scenarios. In Sweden, a climate factor of 1.2 is commonly advised for hourly precipitation with a 100-year recurrence interval (for more information; svensktvatten.se/Vattentjanster and klimatanpassning.se). Another approach is to incorporate assessed non-stationarity into the IDF-concept. Cheng and AghaKouchak (2014) propose a method addressing changes in precipitation intensity, duration and frequency analysis [2, 8, 9, 18, 21, 27, 36, 53, 54] and provide an approach that customizes the adjustment of design storms to local climate change. Their method, Non-stationary Extreme Value Analysis (NEVA), accounts for non-stationarity in climate time series, e.g. for precipitation [70], and includes methods for addressing temporal changes in extremes [10, 24, 23, 32, 56, 62, 69, 72]. For IDF-curves, the method uses a General Extreme Value (GEV) distribution fitted to historical annual maximum precipitation and infers the distribution parameters using a Bayesian-based Markov Chain Monte Carlo (MC-MC) approach [8]. The estimated intensities (return levels) for particular recurrence intervals (return periods) are determined along with uncertainty bounds, assuming that climate change cause the distribution characteristics for climatic extremes to change linearly with time. A case study on ground-based precipitation data in the U.S. where extreme precipitation increases over time, shows that stationary IDF-curves can underestimate extreme precipitation events by as much as 60 % on an hourly scale. Consequently, structures designed to withstand extreme events estimated assuming stationarity may not resist extreme events under climate change [7]. NEVA provides an approach to estimate design storms assuming non-stationary conditions based on local historical information about extreme precipitation patterns.

The main goal of this study was to determine if the influence of climate on extreme precipitation in Sweden should be considered when deriving design storms, by means of representing the climate change with the concept of non-stationarity. Non-stationarity is here assumed to be a linear increase in extreme precipitation over time. We also investigate the effect of assuming non-stationary conditions i eestimating design storms for locations where extreme precipitation events are influenced by climate change.

Chapter 2

Method

Records of ground based data from 139 Swedish automatic weather stations over approximately 50 years provided the historical information about precipitation patterns. The time series were collected from the Swedish Hydrological and Meteorological Institute's (SMHI) open database and no corrections were made for potential biases from the measuring instrument. The highest observed precipitation events within every water year (October 1 to September 30) for different durations (1-day, 2-day, 3-day...7-day) were extracted from the data records. Those locations exhibiting a trend over time, detected with the Mann-Kendall trend test, were used to develop IDF-curves assuming non-stationary and stationary conditions. It was assumed that extreme precipitation events increase linearly with time due to climate change and also that historic hydrometeorological conditions can be used to characterize the future. Return levels corresponding to the return periods of 10, 25 and 50 years were derived with NEVA software package [8]. No corrections were made for potential cyclical patterns caused by the North Atlantic Oscillations (NAO). This chapter summarizes the data collection, quality control and analysis of trends and change in distribution of the data records. A detailed description of the return level derivation, the parameter estimation with NEVA and the simulation strategy follow. Finally, the development of the IDF-curves is disclosed. All analyses and simulations were performed in Matlab. The maps were produced by means of Lantmateriets open database for Swedish mapping and QGIS.

2.1   Study Site

Sweden, located in northern Europe, has a mild climate relative to its high latitude because of its proximity to the Atlantic Ocean and the dominating wind directions. Low pressure systems supply the region with precipitation all year round. However, long periods dominated by dry climate may occur when high pressure systems block the low pressure systems north and south of Sweden. The south Sweden coast is warm temperate whereas most of the land mass is considered cold temperate. The temperature varies strongly with seasons. During the winter, wind, wind speed and cloud cover highly impacts temperatures. The valleys experience the lowest temperatures. Conversely, in summer the lowest temperatures are measured at mountain

peaks. The total annual precipitation ranges between 1000 and 2000 mm. Several factors affect precipitation patterns: e.g. topography and atmospheric circulation patterns. As wind blows in over the high mountains in the northwest, air is forced upwards and cools, causing the largest precipitation in the country (2000 mm per year). In the same regions, there are locations with little precipitation, areas of so-called rain shadow (300 mm per year). In southern Sweden, the highland in the southwest receives the most precipitation. Large amounts of precipitation also hit the northeast coast. The archipelago experiences less precipitation compared to inland areas. (Kunskapsbanken at SMHI.se).

2.2   Data collection and Processing

Daily precipitation data were collected from the SMHI's database for 139 weather stations in Sweden. The record length varied among the stations but all cases covered at least 50 years, missing years excluded. Only records with at least 350 days per year and less than 5 missing years in total were included in the study. No data were removed which means that a potential bias was introduced into the analysis. Time series for durations of 2-7 days were created based on the daily precipitation data. Daily values for every water year were summarized using a moving window, i.e. day 1 and 2 as well as day 2 and 3 are summed [3, 16]. The annual maximum precipitation in each successive water year was also extracted from the time series (figure 2.1) [7].
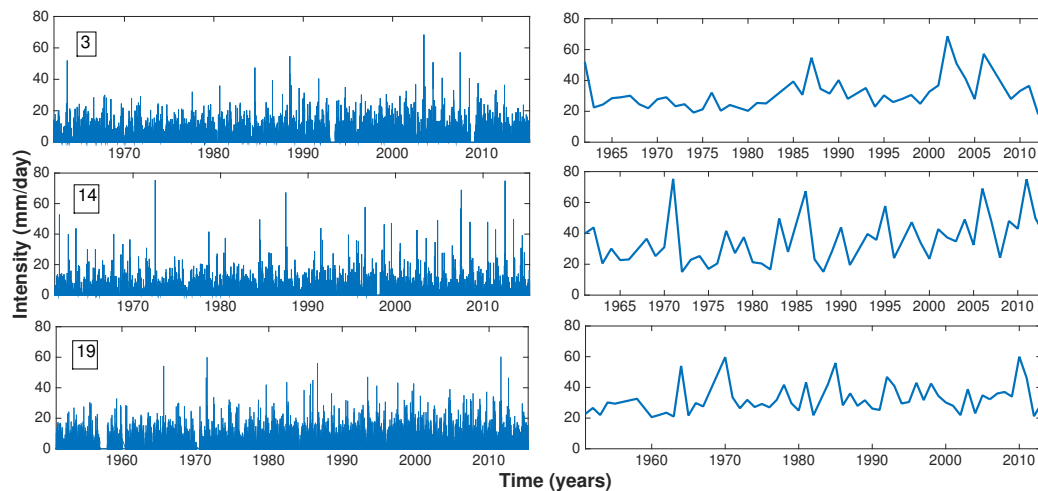

Figure 2.1: The full record of daily precipitation (left) and the daily annual maximum precipitation (right) for station 3, 14 and 19 table 2.1. The annual maximum 1-day, 2-day, 3-day...7-day precipitation events are used for trend and frequency analysis to develop IDF-curves at locations exhibiting an increasing trend over time.

Tabell 2.1: 21 out of 139 stations that held a trend in daily annual maximum precipitation presented with position (longitude, latitude), total annual precipitation (AS) and annual mean precipitation (AM).

Number	Station Name	Longitude	Latitude	AS (mm)	AM (mm/d)		
					1-day	4-day	7-day
1	Charlottenberg	59.8875	12.3039	770	38.2	15.0	10.7
2	Kasa D	63.3266	19.0532	702	36.8	15.4	11.1
3	Ljungby D	56.8099	13.9694	777	31.3	13.4	9.7
4	Lövberga D	63.9664	15.8533	559	28.7	12.3	8.9
5	Myskelåsen D	62.3355	12.647	612	32.2	13.3	9.5
6	Nävelsjö	57.4397	14.8863	671	33.6	13.0	9.0
7	Prästkulla	57.7242	14.986	703	34.3	13.5	9.7
8	Rossared D	57.485	12.1997	930	37.4	15.8	11.9
9	Rörvik D	57.2377	14.5751	723	34.8	13.8	9.7
10	Saittarova	67.3345	22.2433	566	30.8	12.3	8.4
11	Skillingaryd	57.4302	14.1004	833	32.5	14.1	10.4
12	Åby	56.9152	14.0141	733	32.3	13.5	9.6
13	Åtorp	59.0966	14.3678	709	33.6	13.9	10.3
14	Ödeshög D	58.2307	14.6624	580	35.6	13.9	9.3
15	Säffle	50.1412	12.9359	742	39.6	16.6	11.7
16	Söraby	57.0345	14.9446	679	33.2	13.4	9.3
17	Svinhult D	57.7471	15.3914	680	37.6	14.6	10.2
18	Tvingelshed	56.3254	15.5793	700	36.2	14.2	10.0
19	Varberg	57.1084	12.2741	765	32.6	13.8	10.0
20	Vänersborg	58.3552	12.3616	7767	33.0	14.4	10.5
21	Mariestad	58.7136	13.823	568	33.8	13.2	9.0

2.3 Trend Analysis and change in distribution

2.3.1 Mann-Kendall trend test

The Mann-Kendall (MK) trend test was used to detect trends in annual maximum precipitation over time for 1-day, 2-day, 3-day...7-day precipitation events[7]. A trend occurs if the investigated variable consistently decreases or increases over time. There are various methods to evaluate trends in data, including parametric and non-parametric. A parametric method requires an underlying distribution, e.g. the commonly used linear regression assumes data to be normally distributed. The Mann-Kendall trend test is a non-parametric method, i.e. the analyzed data do not need an underlying distribution, which makes it useful for extreme value analysis.The significance level was set to 0.05, a level typically applied within hydrology [28]. This means that the data are inconsistent with the null hypothesis if the p-value is equal to or below 0.05. The null hypothesis in the Mann-Kendall trend test is that there is no trend in data. [28, 37].

The MK-test analyzes the sign of the difference between successive data points. Each observation is compared with earlier observations, resulting in n(n-1)/2 possible data pairs (n is the total number of observations). An observation can be declared as equal to, less than or greater than another observation and is assigned a value of 1, 0 or -1. The test statistics (S) is the sum of the integers and if large and positive, later observations tend to be larger than earlier observations, i.e. an upward trend is indicated. If S is large and negative, a decreasing trend is indicated. If S is small there is no trend. [28]

Only stations show an increasing trend on a daily scale were analyzed in NEVA.

2.3.2 Two-Sample Kolmogorov-Smirnov test

We used the two-sample Kolmogorov-Smirnov test to investigate if there was a change in distribution between the first and second half of the annual maximum precipitation at the different stations. The test is, like the Mann-Kendall trend test, a non-parametric hypothesis test. It evaluates the difference between the cumulative distribution functions for the two parts of the data record. If the null hypothesis is rejected, the two distribution functions of annual maximum precipitation are considered to come from different distribution functions, indicating that the precipitation characteristics have changed. In this study, the Matlab-function kstest2.m was used. [28]

$$D = max_x\left(\left|\hat{F}_1(x) - \hat{F}_2(x)\right|\right) \tag{2.1}$$

2.4 Frequency Analysis with NEVA

The Nonstationary Extreme Value Analysis (NEVA) software package was developed by Linyin Cheng, Amir AghaKouchak, Eric Gilleland and Richard W Katz in 2014 to facilitate extreme value analysis under both stationary and non-stationary assumptions. NEVA estimates return levels, return periods and risks of climatic extremes with Bayesian inference The extreme value parameters are estimated with a Differential Evolution Markov Chain (DE-MC) approach for global optimization over the parameter space. NEVA includes posterior probability intervals (uncertainty bounds) of estimated return levels through Bayesian inference, with its inherent advantages in uncertainty quantification. The software presents the results of non-stationary extreme value analysis using the general extreme value distribution fitted to time series of annual maximum precipitation. Previous studies have used NEVA on temperature and precipitation data in the United States. [7, 8]

2.4.1 Return period and Return level

In this study, the highest precipitation intensity estimated within a certain time interval and location was assessed with the return level (q_p) and return period (T) concept, a common sta-

tistical measurement in hydrological risk analysis [**?**]. The concept can be illustrated by defining a T-year return level, i.e. a certain precipitation intensity, with the annual maxima exeedance probability $(1 - p$, where p is the non-exceedance probability) of $1/T$. Hence, a certain event's return period is the inverse of the probability that the event will be exceeded in any given year (equation (2.2)). For example, a 100-year return level has the exceedance probability of 1 %. In this way, the return level (the quantile) can be related to the return period (the associated time interval), as in this study with the General Extreme Value (GEV) distribution function, see equation (2.3). [8, 9]

$$T = \frac{1}{1 - p} \tag{2.2}$$

$$q_p = \left(\left(-\frac{1}{lnp} \right)^{\xi} - 1 \right) * \frac{\sigma}{\xi} + \mu, (\xi \neq 0) \tag{2.3}$$

$\theta = (\mu,\ \sigma,\ \xi)$ are the distribution parameters, describing the shape of the GEV distribution function wherein the return levels and associated return periods are estimated. μ is the location parameter and specifies the center of the distribution, σ is the scaling parameter and determines the distribution's deviation about the location parameter, ξ is the shape parameter governing the tail behavior, i.e. representing the most extreme precipitation events' effects on the frequency distribution of the annual daily maximum precipitation events.

The return level and return period described in equation (2.2) and equation (2.3) assume stationarity, meaning the return level of a particular return period is the same for all successive years. This implies that the statistical properties, $\theta = (\mu,\ \sigma,\ \xi)$, are time-invariant. However, in the non-stationary case provided by NEVA the distribution parameters are time-variant, meaning that the properties of the distribution will vary through time [44]. As in previous studies, the location parameter μ was assumed to be a linear function of time (equation (2.4)) [8, 17, 30, 51]. At some stations, the scale parameter was also set to be time invariant to improve model performance (equation (2.5)). μ_1, μ_0, σ_1 and σ_0 are the regression parameters estimated from the posterior distribution and used to derive $\tilde{\mu}$ and $\tilde{\sigma}$ from the median and 95th percentiles of the quantiles (Q_κ, where κ is the percentile), i.e. $\mu(t{=}50)$ and $\mu(t{=}95)$ since $t_{max}{=}$ 100 [8]. The median is referred to as medium risk because $\tilde{\mu}$ are estimated for the climate conditions 50 years into into the future. The 95th percentile is referred to as the low risk since $\tilde{\mu}$ is estimated for the climate conditions 95 years into the future, and is thus equivalent to a more extreme climate. This basically means that equation (2.3) can be rewritten into equation (2.6).

$$\tilde{\mu} = Q_\kappa(\mu_{t_1}, \mu_{t_2}, ...), \mu(t) = \mu_1 t + \mu_0 \tag{2.4}$$

$$\tilde{\sigma} = Q_\kappa(\sigma_{t_1}, \sigma_{t_2}, ...), \sigma(t) = \sigma_1 t + \sigma_0 \tag{2.5}$$

$$q_p = \left(\left(-\frac{1}{lnp} \right)^\xi - 1 \right) * \frac{\tilde{\sigma}}{\xi} + \tilde{\mu}, (\xi \neq 0) \tag{2.6}$$

Extreme Value Theory

Extreme Value Theory (EVT) provides methods for analyzing climatic extremes and their return levels. One approach within EVT is to derive block maxima series and fit a continuous probability distribution to them, e.g. the General Extreme Value (GEV) distribution is fitted to the annual maximum precipitation for different durations. A probability distribution describes the probability of an outcome within a sample space, e.g. the probability of climatic extremes within a 50-year return period. The GEV distribution comprises three simpler distributions, commonly used within EVT, into one (equation (2.7)). The functions Gumbel, Frechet and Weibull are also known as the Type I, II and III extreme value distributions. GEV allows a continuous range of possible distribution shapes and therefore allows the data to decide the most appropriate one, i.e. the GEV will converge to either distribution. If ξ, from the distribution parameter set up $\theta = (\mu, \sigma, \xi)$, approaches zero, the data converges to Gumbel distribution characterized by exponentially decreasing tails. If ξ is negative, the data will fit the Weibull distribution wherein the tails decrease as a polynomial. The data will approach the Frechet distribution if ξ is greater than zero, i.e. the tails are finite [8]. The tails represent the historical data's most extreme values and the GEV's asymptotic justification is particularly useful for extrapolating beyond the range of the data [9]. The cumulative distribution function can be expressed as equation (2.7) and has a solution if $(1 + \xi(\frac{x-\mu}{\sigma})) > 0$.

$$\Xi(x) = \exp\{-(1 + \xi(\frac{x - \mu}{\sigma}))^{\frac{-1}{\xi}}\} \tag{2.7}$$

2.4.2 Parameter estimation in NEVA: Bayesian inference

NEVA uses Bayesian inference to estimate the posterior distributions the probability distribution of an unknown quantity of the parameters $\beta_1 = (\mu_1, \mu_0, \sigma, \xi)$, $\beta_2 = (\mu_1, \mu_0, \sigma_1, \sigma_0, \xi)$ and $\theta = (\mu, \sigma, \xi)$ [8]. The inference is based on Bayes theorem, a probability theory theorem used for determining conditional probabilities, in other words, the probability of an outcome given another outcome. The posterior distributions are estimated based on knowledge of the prior distribution
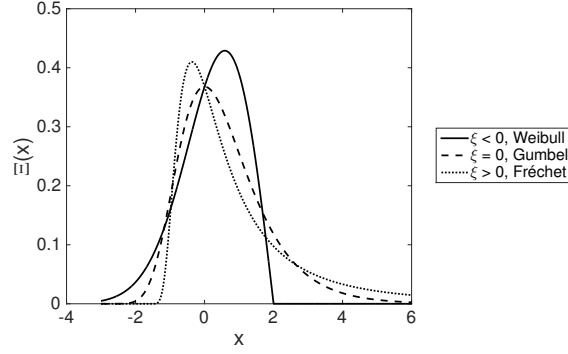
Figure 2.2: The General Extreme Value (GEV) distribution for the case of Weibull (solid line), Gumbel (dashed line) and Frechet (dotted line) distributions. The GEV has a function value, $\Xi(x)$, for all x. The shape of the GEV is determined by the parameters $\theta = (\mu, \sigma, \xi)$. If $\xi < 0$, GEV converges to Weibull distribution, meaning the tails of the distribution decrease exponentially. If $\xi = 0$, GEV converges to Gumbel distribution and the tails of the distribution converge as a polynomial. If $\xi > 0$, GEV converges to the Frechet distribution, meaning the tails of the distribution are finite.

and the observation vector, $\vec{y} = (y_{t=1:N_t})$, where N_t is the number of observations. The prior distribution, $p(\beta|x)$ and $p(\theta)$, aim to encode prior knowledge of the parameters by restricting the possible range of parameters of a GEV distribution based on information from relevant case studies. The information from historical data is quantified using the likelihood concept, i.e. the probability to observe what has actually been observed. Assuming independence between observations, the likelihood corresponds to the joint pdf of a random vector calculated as the product of its marginal pdfs, (equation (2.8) and equation (2.10)). This requires that the prior distribution is specified. This study uses the default prior distributions provided by NEVA, i.e. the non-informative normal distributions for the location and scale parameters and a normal distribution with a standard deviation of 0.3 for the shape parameter. The historical data and the prior distribution are used to estimate the posterior distribution through multiplication, equation (2.8) and equation (2.10), where $x(t)$ denotes the covariate values of the parameters $\beta_\lambda = (\beta_1, \beta_2)$ under the non-stationary assumption. The posterior distribution provides information about the parameters for estimating return levels. [51]

$$p(\beta_\lambda|\vec{y}, x) \propto p(\vec{y}|\beta_\lambda, x)p(\beta_\lambda|x) \tag{2.8}$$

$$p(\vec{y}|\beta_\lambda, x) = \prod_{t=1}^{N} p(y_t|\beta_\lambda, x(t)) = \prod_{t=1}^{N} p(y_t|\mu(t), \sigma(t), \xi) \tag{2.9}$$

$$p(\theta|\vec{y}, x) \propto p(\vec{y}|\theta, x)p(\theta|x) = \prod_{t=1}^{N} p(y_t|\theta)p(\theta) \tag{2.10}$$

10

The Differential Evolution Markov Chain (DE-MC) is used to optimize over parameter space. This means that the DE-MC provides a large number of realizations from the parameter joint posterior distributions and allows estimation of the median and the 95th percentile of the $\mu(t)$ and $\sigma(t)$. The DE-MC is based on the Markov Chain Monte Carlo method (MC-MC). The MC-MC generates a random walk in which the asymptotic distribution is the posterior distribution. MC-MC uses another distribution called the proposal or jump distribution to propose candidate values for the posterior distribution. The candidate values are then accepted or rejected, according to a given acceptance rule. NEVA uses the method criterion $\hat{R}$ to assess convergence of the sampling approach and is set to 1.1. For further reading on this topic see Cheng and AghaKouchak (2014) [8].

2.4.3 Simulation strategy in NEVA

Given the distribution parameters' distributions, the return levels for 10-, 25- and 50- year return periods were estimated from values generated from equation (2.6). Annual maximum precipitation data records from stations holding trends in time (table 2.1) were used for the simulations in NEVA. The non-stationary return levels were estimated with location and scale parameters corresponding to future climate conditions: 50th percentile of the parameter distribution (hereafter, medium risk); and 95th percentile of the parameter distribution (hereafter, low risk). To start, only the location parameter was set as time-invariant, but to improve model performance the scale parameter was also allowed to be time-invariant. The default prior distributions suggested by NEVA were applied (table 2.2) [8]. The number of evaluations was set to 50 000. The median of the ensemble of simulations were used to estimate return levels and the 5th and 95th percentiles described the uncertainty bounds.

The model's performance using the NEVA output was assessed by comparing the estimated and empirical return levels. The empirical return levels were calculated from the empirical cumulative distribution function derived for each station, and inserted into equation (2.2). If the empirical values laid within the ensemble, the simulation was considered good. The posterior distributions of the parameters were compared with the normal distribution to check the simulation's convergence. In the stationary case, the quantile quantile plot (QQ-plot) between observed annual maximum precipitation and theoretical values was also analyzed to examine the fit of the model.

The model performance improved for stations 5, 7, 9, 12 and 18 when both $\mu(t)$ and $\sigma(t)$ were set as time-invariant. Two time-invariant distribution parameters were only applied to 1-day precipitation events.

Table 2.2: The range of parameters in the GEV distribution allowed for the prior distributions. The intervals are the default settings in NEVA. σ and β are the scale and shape parameters, σ_1, σ_0, μ_1 and μ_0 are the regression parameters for the time-invariant location and scale parameter. Either σ or σ_1 and σ_0 were applied.

Parameter	Lower boundary	Upper boundary
σ	0	100
β	0	0.3
μ_1	0	100
μ_0	0	100
σ_1	0	10
σ_0	-100	100

2.5 Intensity Duration Frequency Curves

Intensity Duration Frequency (IDF) curves were developed for 10-, 25- and 50-year return periods. The estimated return levels were plotted against duration for the non-stationary and stationary assumption respectively. The return levels are estimated from the median of the ensemble generated by NEVA while the 5th and 95th percentile constituted uncertainty bounds (section 2.4.2 and section 2.4.3)

Chapter 3

Results

3.1 Trend Analysis and change in distribution

Of the 139 stations surveyed, 20 stations showed positive trend in time (p-value was lower than 0.05) and 1 station showed a negative trend (station 13) for daily annual maximum precipitation (table 6.1 in appendix). The significance level was low in general. For precipitation on a multi-daily scale (2-day, 3-day...7-day) more stations had increasing trends for higher durations (figure 3.1). However, only 12 stations had a trend through all durations. These stations (station 3, 4, 7, 8, 9, 11, 12, 14, 16, 17, 19 and 20) (table 2.1 in section 2.2) were further investigated.
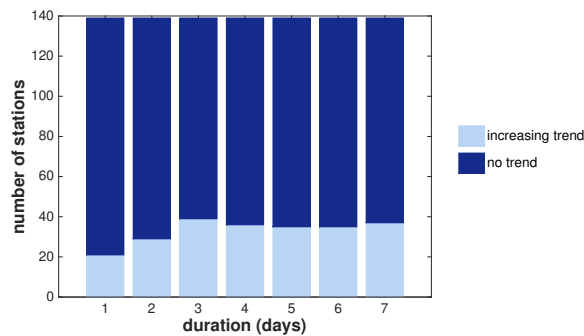

Figure 3.1: Proportion of stations showing a significant trend (p=0.05) in annual daily maximum precipitation. The trends are tested with the Mann-Kendall trend test. 20 stations showed trend for daily resolution, while 29, 39, 36, 35, 35 and 37 stations showed increasing trends for 2-day, 3-day,... 7-day precipitation events.

The cumulative distribution function (cdf) for the second part of the investigated time interval, the last 25 years approximately, showed higher intensities than the first interval at all stations and also showed an increase in annual maximum precipitation (figure 3.2). The difference in distribution between the first and second part of the 50 years was significant only for a fraction of the stations with increasing trends in annual maximum precipitation (figure 3.3, figure 3.4, figure 3.5, figure 3.6).
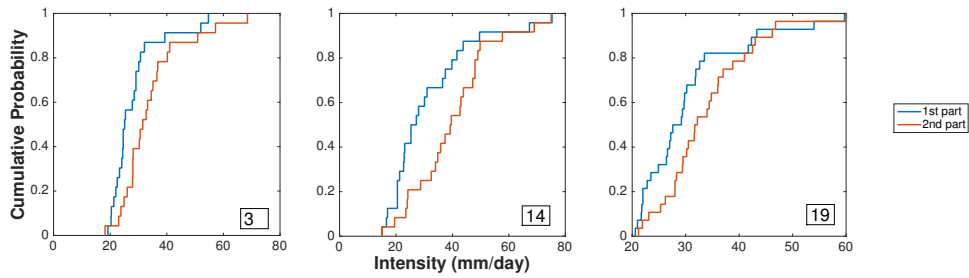
Figure 3.2: The change in cumulative distribution function of the daily annual maximum precipitation for station 3, 14 and 19. The distribution shifted forward in all three cases, meaning that higher intensities have become more frequent during the last 25 years.
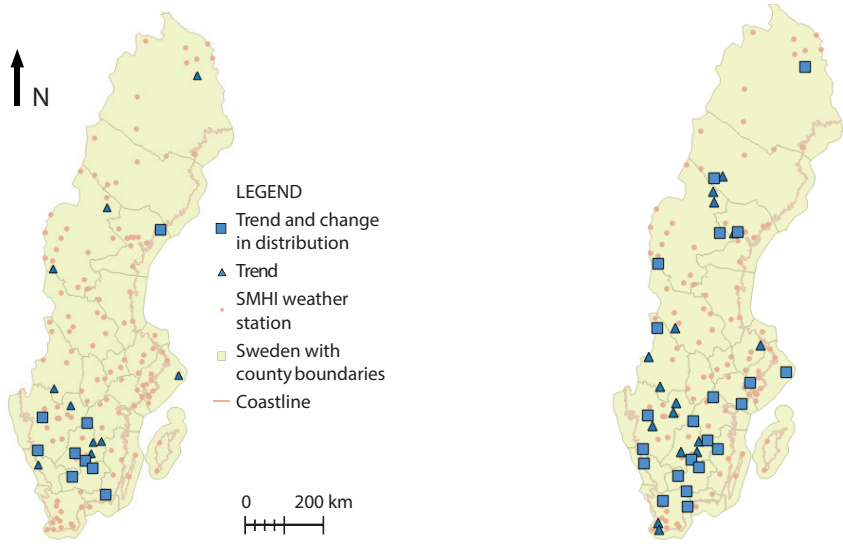
Figure 3.3: Daily annual maximum precipitation; Stations with increasing trend (20) and change in distribution (15).

Figure 3.4: 3-day annual maximum precipitation; Stations with increasing trend (36) and change in distribution(23).

Figure 3.5: 5-day annual maximum precipitation; Stations with increasing trend (35) and change in distribution (20).

Figure 3.6: 7-day annual maximum precipitation; Stations with increasing trend (37) and change in distribution (23).

3.2 Daily return levels estimated with NEVA

The median of the return levels derived with NEVA represent the estimated return levels for particular return periods assuming stationary (figure 3.7) and non-stationary conditions (figure 3.8). The empirical values indicate the performance of the model and as can be seen for station 3, (figure 3.7 and figure 3.8) they was within the ensemble. In figure 3.9 and figure 3.10, non-stationary return levels were estimated with parameters for conditions 50 years (medium risk) and 95 years (low risk) into the future, respectively.
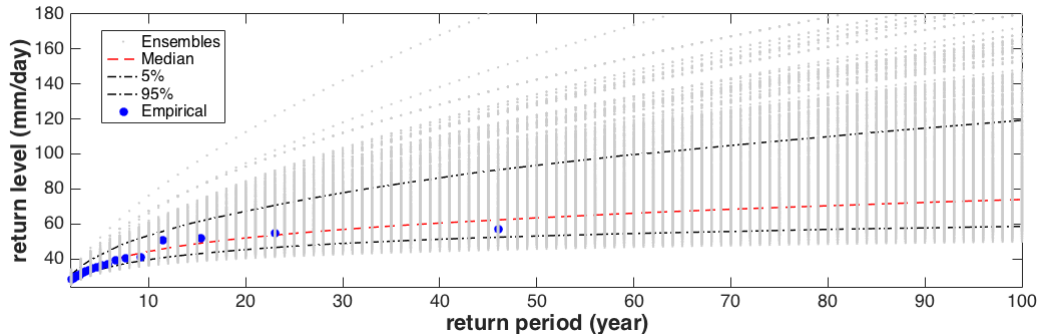

Figure 3.7: Stationarity; highest daily precipitation (return level; mm/day) versus recurrence interval (return period) for station 3 estimated with the NEVA software package. Points are observed values and lines are estimated values. The grey colored ensemble are the return levels' realizations for the corresponding return period. The median, 5th and 95th percentiles are calculated within the ensemble for each return period.
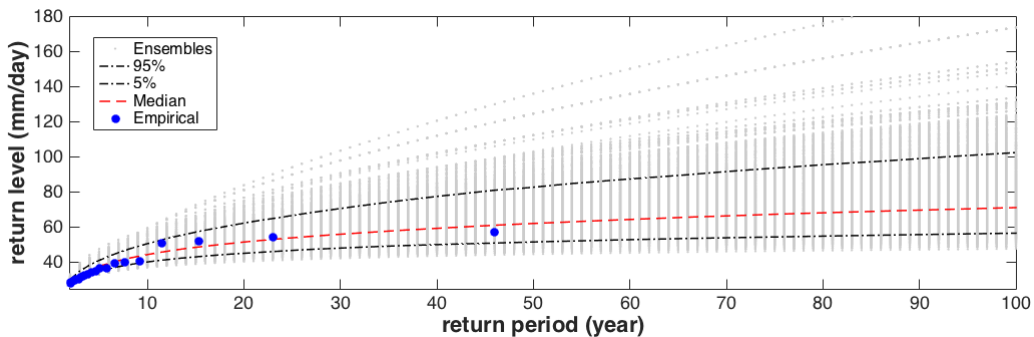
Figure 3.8: Non-stationarity (1963-2013); Highest daily precipitation (return level; mm/day) versus recurrence interval (return period) for station 3 estimated with the NEVA software package.The grey colored ensemble are realizations of the return levels for the corresponding return period. The median, 5th and 95th percentiles are calculated within the ensemble for each return period.

Almost all stations with increasing trends showed positive absolute and relative differences between return levels estimated assuming non-stationary and stationary conditions, respectively, (figure 3.11, figure 3.12) for a 25-year return period. The relative difference ranges from 7 % to just over 55 % (medium risk) and 9 % to 77 % (low risk). Station 8 has the largest absolute difference; 27 mm/day (medium risk). The relative difference between non-stationary and sta-
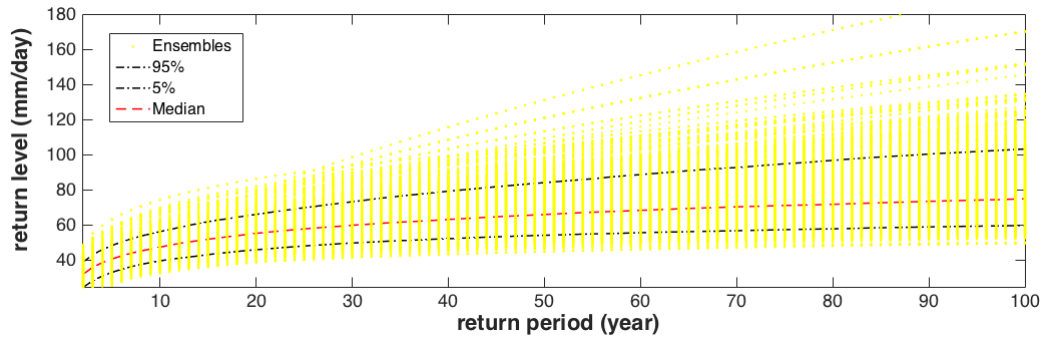
Figure 3.9: Non-stationarity return levels (medium risk) of daily precipitation (mm/day) versus recurrence interval (return period) estimated with the NEVA software package. The yellow lines are the estimated values based on the 50th percentile of parameter distribution). The median, 5th and 95th percentiles are calculated from the ensemble of estimates for each return period.
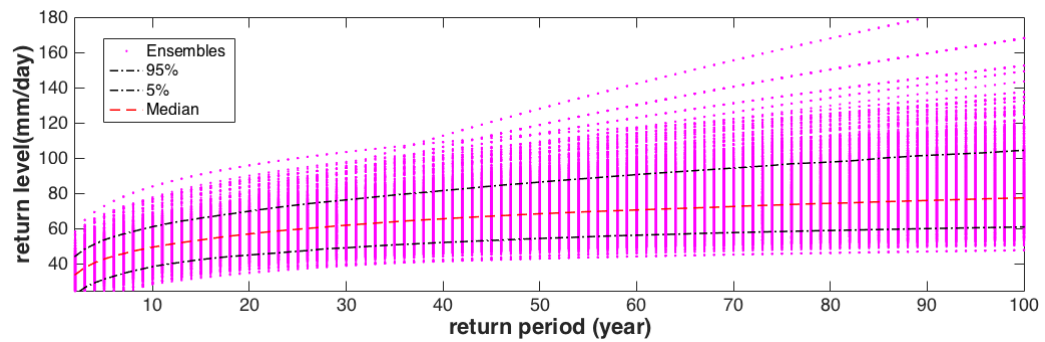
Figure 3.10: Non-stationarity return levels (high risk) of daily precipitation (mm/day) versus recurrence interval (return period) estimated with the NEVA software package. The yellow lines are the estimated values based on the 95th percentile of parameter distribution). The median, 5th and 95th percentiles are calculated from the ensemble of estimates for each return period.

tionary return levels (medium risk) for 10- and 50-year storms are found in table 3.1 (for low risk see appendix)
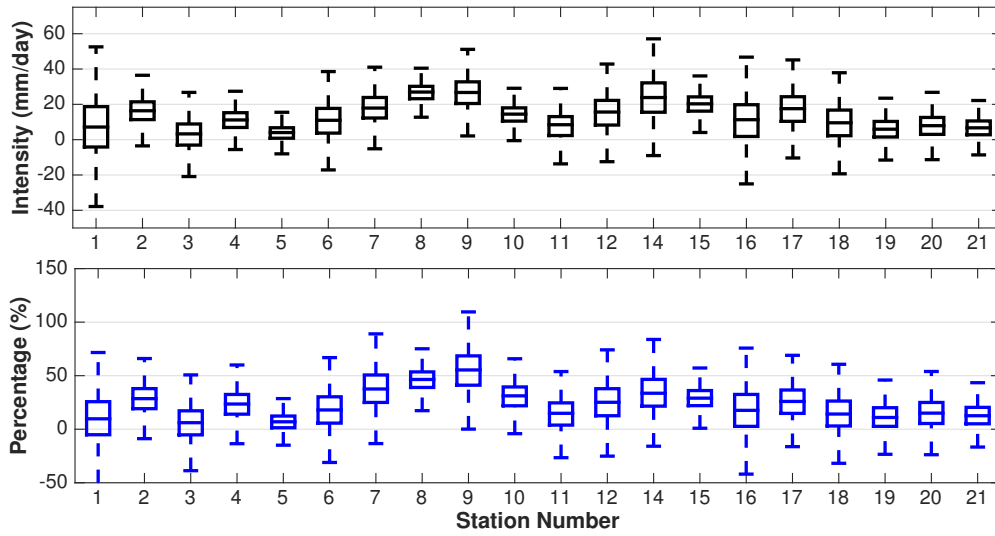
Figure 3.11: Medium risk, the absolute difference between the highest daily precipitation (return level; mm/day) for a return period of 25 years, estimated assuming non-stationary and stationary conditions, respectively (upper graph), for the 20 stations with significant increasing trends in daily annual maximum precipitation. The lower graph shows relative difference (%). Station 8 has the largest difference between non-stationary and stationary return levels.

Figure 3.12: Low risk, the absolute difference between the highest daily precipitation (return level; mm/day) for the return period of 25 years, estimated assuming non-stationary and stationary condition respectively (upper graph), for the 20 stations with increasing trends in time. The lower graph shows relative difference (%). Station 8 has the largest difference between non-stationary and stationary return levels.

Table 3.1: Medium risk; The relative difference between the highest daily precipitation (return level; %) for 10- and 50-year return periods, estimated assuming non-stationary and stationary conditions, respectively, for the 20 stations with increasing trends in time. The medians (p_{50}) are boldfaced, representing the estimated return level, while the 5th and 95th percentile (p_5 and p_{95}) constitute uncertainty bounds.

| T	10 yr			50 yr		
Station	p_5	p_{50}	p_{95}	p_5	p_{50}	p_{95}
1	-14.8	**9.7**	37.4	-36.5	**7.5**	67.5
2	10.7	**34.4**	58.2	-2.7	**24.1**	51.6
3	-17.2	**7.2**	31.5	-32.0	**3.2**	40.2
4	2.5	**26.7**	46.8	-10.5	**20.7**	45.4
5	14.5	**29.5**	42.1	6.2	**25.9**	40.0
6	-7.8	**23.8**	52.7	-30.2	**12.4**	51.8
7	-15.0	**11.6**	41.2	-28.1	**0.1**	29.6
8	33.4	**53.4**	71.6	17.2	**42.0**	59.9
9	-6.4	**22.5**	50.3	-32.1	**-1.9**	35.2
10	14.4	**34.3**	54.8	4.0	**28.7**	53.1
11	-2.4	**17.2**	38.1	-21.9	**10.7**	41.6
12	-1.3	**30.1**	62.7	-32.4	**2.2**	43.4
14	13.2	**44.2**	78.6	-7.4	**25.5**	61.8
15	11.7	**31.1**	52.9	0.1	**27.0**	48.4
16	-1.8	**24.1**	49.7	-34.5	**11.3**	59.1
17	5.7	**29.8**	53.9	-7.4	**22.1**	54.4
18	8.3	**33.7**	62.8	-15.6	**18.2**	45.7
19	-3.7	**14.0**	31.4	-21.8	**7.9**	38.6
20	-1.1	**17.9**	38.6	-18.1	**12.3**	48.1
21	-6.0	**8.5**	22.8	-4.8	**16.2**	47.2

3.3 Multi-daily return levels estimated with NEVA

Non-stationary return levels are estimated to be higher than stationary return levels among the investigated stations, for different durations and return periods. However, the magnitude of the difference between them varies. At station 3, the size of absolute and relative differences increases with increasing duration (figure 3.13). Station 14 and 19 show decreasing absolute difference with increasing duration, while the relative difference does not change consistently with increasing duration (figure 3.14). In table 3.3 and table 3.2 various patterns in absolute and relative difference are indicated, depending on duration among the locations. Further, the absolute and relative differences decrease with increasing return level, except for station 3, where the absolute difference increases slightly (figure 3.13 and figure 3.14). The uncertainty bounds increase with increasing return period.
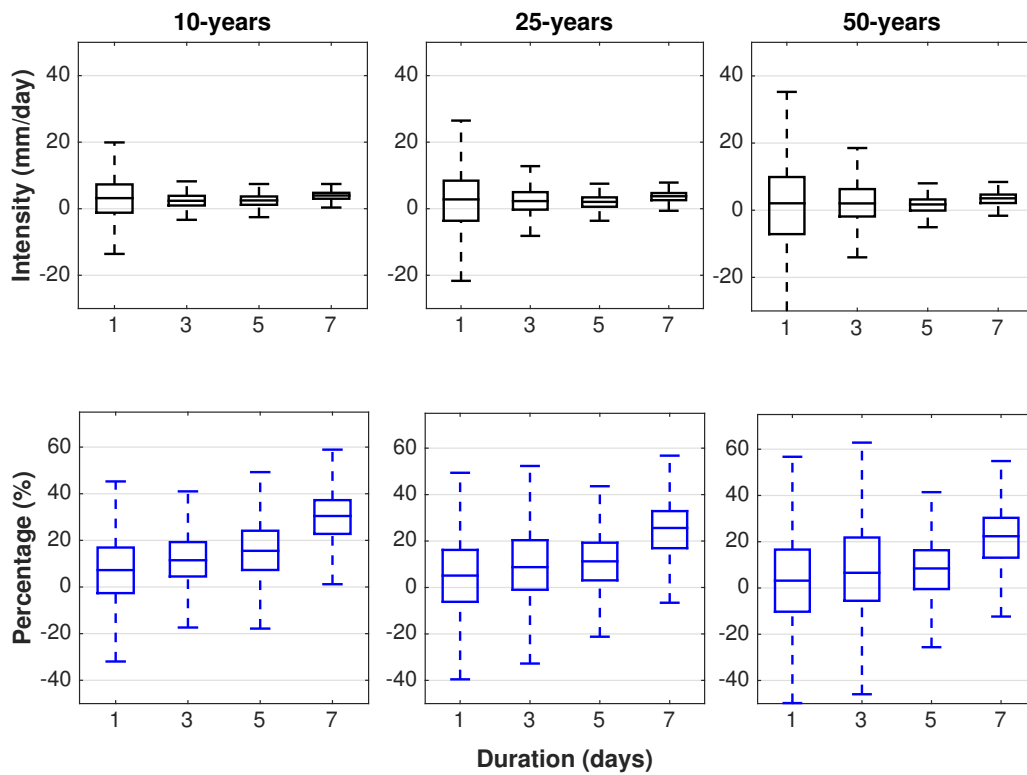
Figure 3.13: Station 3, the absolute difference between the highest daily precipitation (return level; mm/day) for 10-, 25- and 50-year return periods, estimated assuming non-stationary and stationary condition respectively (upper graph) for the medium risk case. The lower graph shows the relative difference (%). Both the absolute and the relative difference increase with duration, but they remain constant with increasing return period.
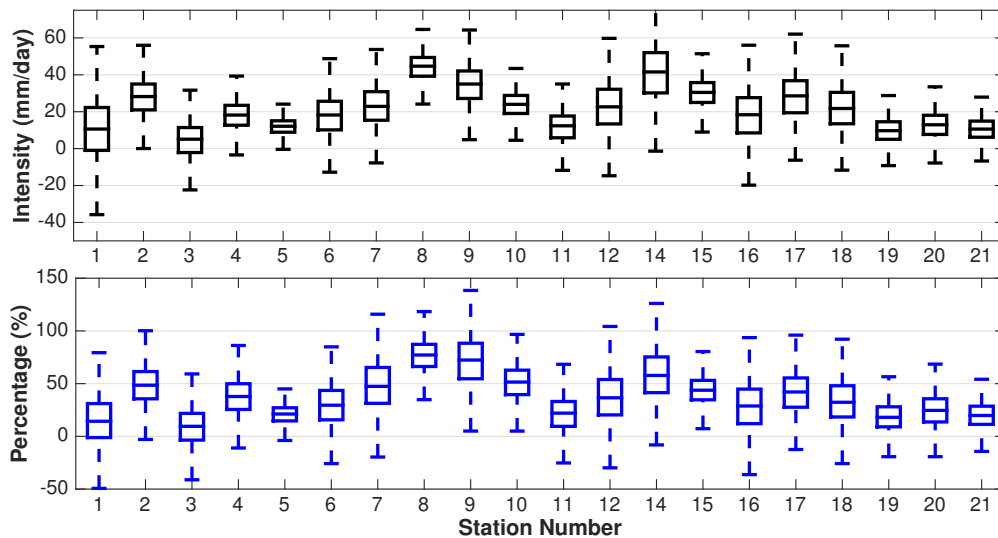
20

Table 3.2: Medium risk, the absolute difference between the highest daily precipitation (return level; mm/day) for a 25-year return period, estimated assuming non-stationary and stationary conditions, respectively. The return levels are estimated for the 12 stations holding a trend for 1, 2, 3, 4, 5, 6 and 7 days. The medians (p_{50}) are boldfaced and represent the estimated return level, while the 5th and 95th percentile (p_5 and p_{95}) constitute the uncertainty bounds.

Duration	3-day			5-day			7-day		
Station	p_5	p_{50}	p_{95}	p_5	p_{50}	p_{95}	p_5	p_{50}	p_{95}
3	-4.0	**2.3**	9.0	-2.0	**2.1**	5.3	0.9	**3.8**	6.3
4	-3.6	**6.6**	14.9	-4.4	**5.0**	9.3	-2.8	**2.5**	8.4
7	-0.9	**5.2**	10.2	-2.8	**2.0**	6.8	-2.0	**1.5**	5.1
8	1.5	**6.2**	11.1	1.9	**5.2**	8.4	0.4	**3.2**	6.1
9	-2.4	**3.8**	11.8	4.1	**8.4**	13.5	-1.9	**2.5**	5.7
11	-2.8	**3.8**	10.1	-1.8	**1.9**	5.3	0.1	**2.6**	5.1
12	-6.1	**3.3**	8.7	-2.1	**3.1**	7.1	4.2	**7.0**	10.8
14	0.0	**7.6**	15.5	3.9	**8.3**	13.3	1.0	**4.7**	9.0
16	-9.1	**4.3**	10.6	-5.5	**2.3**	9.6	-0.4	**2.5**	5.2
17	-0.0	**8.3**	16.0	0.6	**7.0**	11.5	0.7	**4.8**	9.1
19	-1.4	**3.9**	8.5	0.5	**3.5**	6.7	-0.7	**2.2**	4.5
20	4.9	**9.1**	15.3	2.7	**5.0**	7.2	1.1	**4.3**	7.0

Table 3.3: Medium risk, the relative difference between the highest daily precipitation (return level; %) for a 25-year return period, estimated assuming non-stationary and stationary conditions, respectively. The return levels are estimated for the 12 stations holding a trend for 1, 2, 3, 4, 5, 6, 7 days. The medians (p_{50}) are boldfaced and represent the estimated return level, while the 5th and 95th percentile (p_5 and p_{95}) constitute the uncertainty bounds.

| Duration	3-day			5-day			7-day		
Station	p_5	p_{50}	p_{95}	p_5	p_{50}	p_{95}	p_5	p_{50}	p_{95}
3	-12.9	**8.8**	38.4	-9.6	**11.3**	30.1	5.9	**25.6**	44.6
4	-10.2	**24.5**	59.5	-15.4	**25.6**	51.9	-13.2	**14.8**	54.9
7	-2.7	**18.7**	39.7	-12.3	**10.8**	36.4	-11.1	**9.8**	33.4
8	4.9	**22.7**	42.4	9.5	**26.1**	42.6	2.2	**19.7**	37.8
9	-7.5	**12.8**	42.2	17.9	**39.2**	69.3	-10.4	**15.3**	39.1
11	-9.1	**14.6**	40.4	-9.0	**10.4**	29.6	0.4	**17.4**	34.9
12	-17.2	**12.3**	35.9	-9.0	**16.6**	39.3	25.2	**47.1**	74.0
14	0.1	**26.8**	57.4	19.0	**44.8**	74.8	6.3	**30.1**	61.1
16	-20.5	**13.4**	39.4	-19.0	**10.5**	48.8	-2.4	**14.4**	33.6
17	-0.1	**28.1**	57.7	2.3	**31.6**	57.3	4.0	**27.8**	57.5
19	-4.9	**15.5**	35.6	2.6	**19.5**	39.2	-3.8	**14.0**	30.3
20	18.8	**36.3**	61.8	14.5	**27.2**	40.9	6.5	**27.9**	46.1
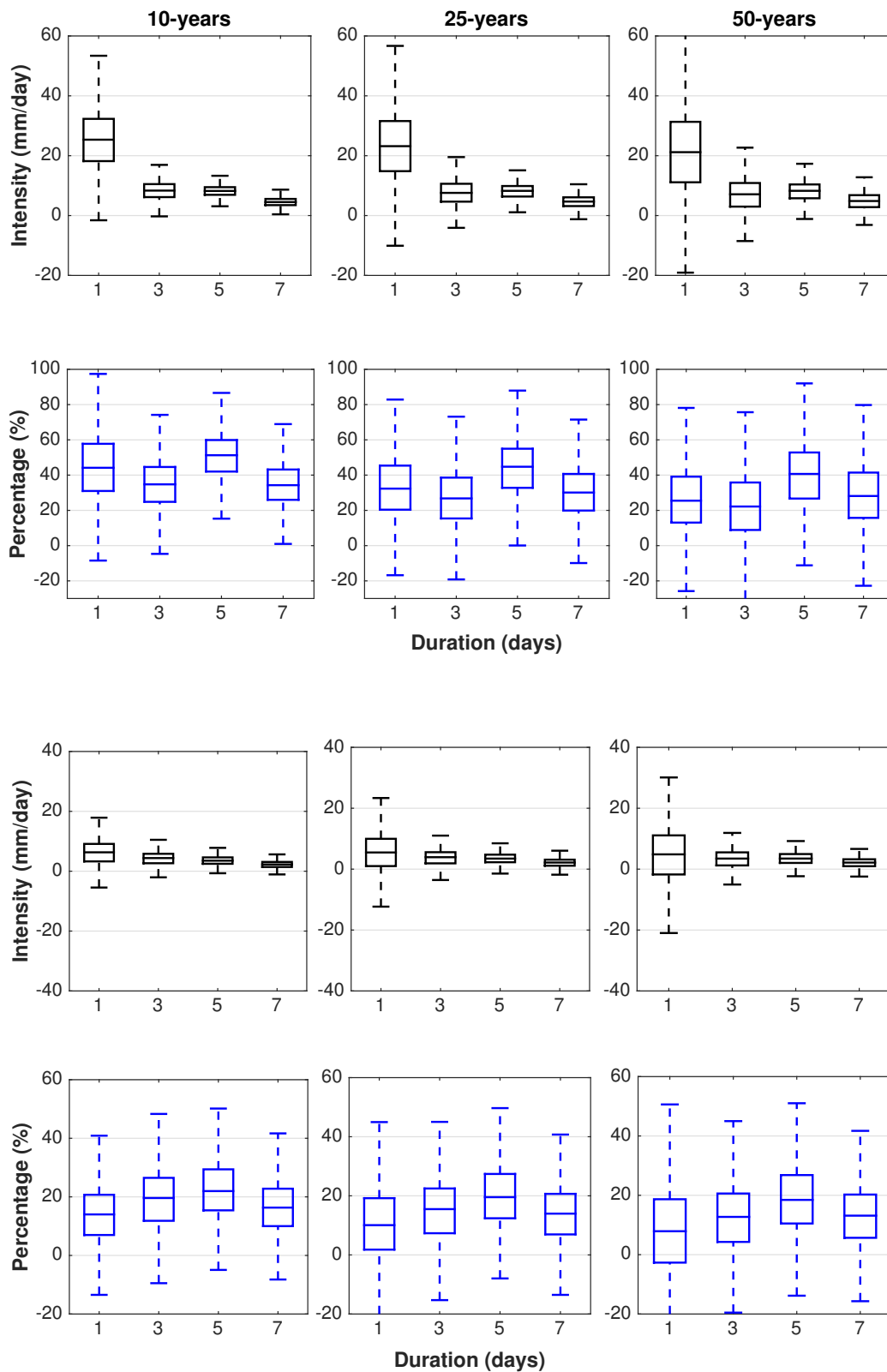
Figure 3.14: Station 14 and 19, the absolute difference between the highest daily precipitation (return level; mm/day) for 10-, 25- and 50-year return periods, estimated assuming non-stationary and stationary condition, respectively (uppermost and third graph for station 14 and 19 respectively), for the medium risk case. The second and lowermost graphs, for station 14 and 19, respectively, show the relative difference (%). Both the absolute and the relative difference increase with duration, but remain constant with increasing return period.

3.4 Intensity Duration Frequency Curves

The design storms estimated from the non-stationary Intensity, Duration, Frequency (IDF) curves exceed the design storms estimated from the stationary IDF-curves. At station 3, the non-stationary IDF-curve predicts a 10-year 1-day storm to be 47.7 mm/day, whereas the stationary IDF-curve predicts the same storm to be 44.2 mm/day. The same design storms for station 14 are 83.3 mm/day and 57.3 mm/day and for station 19, 51.8 mm/day and 25.7 mm/day. The difference is more substantial at low return periods.

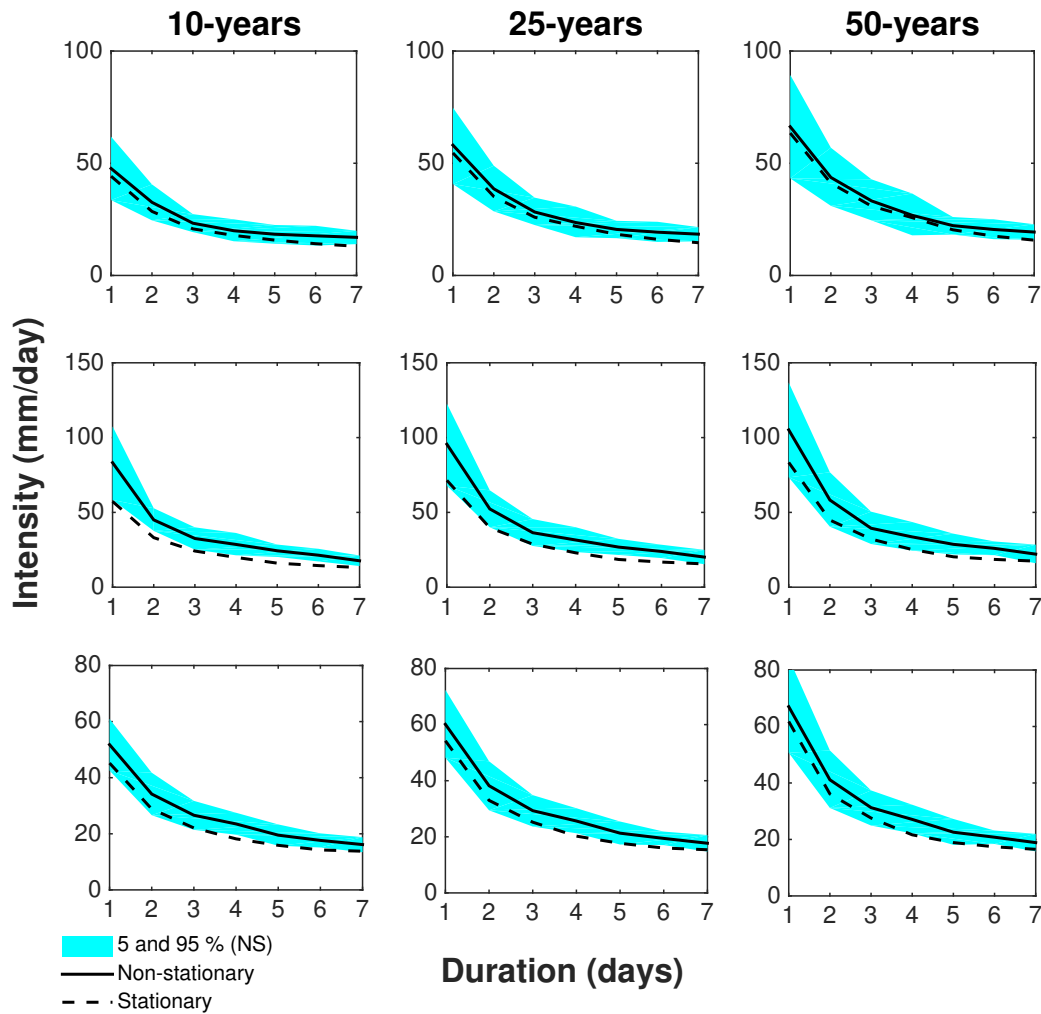Figure 3.15: The non-stationary and stationary IDF-curves for Station 3, 14 and 19. The uncertainty bounds belong to the non-stationary estimates. The stationary IDF-curve is below the non-stationary for all three locations. (Figured generated with help from shadedplot.m (c) 2014 Savyasachi Singh. All rights reserved)

23

Chapter 4

Discussion

For the 20 out of 139 stations showing increasing trends in daily annual maximum precipitation, the return levels estimations under a non-stationary assumption was up to about 50 % higher than return levels estimated under a stationary assumption (figure 3.11). The difference was almost consistent for increasing durations (1-day to 7-day) and return periods (table 6.2 and table 3.2). The fact that increasing trends (section 3.1) in annual maximum precipitation are more common than negative trends supports the suggestion that climate change increases atmospheric moisture [64]. Furthermore, an increase in extreme precipitation events increases the risk of high flows and flooding. The higher estimated return levels for a non-stationary assumption relative to a stationary one indicates the need to consider climate change when constructing design storms in the future [7]. Nevertheless, most locations in this study did not show a trend in annual maximum precipitation over time. The scattered location of the 20 sites with increased return levels indicates that atmospheric circulation patterns as well as local wind and temperature conditions affect extreme precipitation. These aspects are not explicitly considered in this study.

4.1   Trends in annual maximum precipitation

A key result is finding increasing trends in annual maximum precipitation, an indication whether the particular location is affected by climate change in terms of precipitation. The fact that 20 stations out of 139, or approximately 15 %, showed such a positive trend indicates an ongoing climate change concerning extreme precipitation events. This argument is reinforced by the shift into more intense annual maximum precipitation during the last 25 years, which was observed for most of the stations with positive trends. Furthermore, on a multi-daily scale, up to approximately 40 % of the locations showed increasing trends, in line with previous studies demonstrating that Sweden has seen more, longer periods of precipitation extremes due to increased winter rains [3]. The regional trend distribution partly agrees with previous studies in that most of these trends are found in south eastern Sweden, however trends were also observed in the west and north.[3]

The nature of extreme precipitation events is complex: The local atmosphere is highly influenced by global circulation patterns and storm tracks. The Clausius-Clapeyron relationship may not predict extreme precipitation well in regions where circulation change is a major factor, such as mid to higher latitudes [43]. The North Atlantic Oscillation (NAO), which pushes moist air over Sweden with strong westerly winds in its positive phase, is believed to greatly impact extreme precipitation events [55]. NAO has trended towards this phase (strengthened mid-latitude westerlies) over the past three or four decades. [45]

Seasonality also affects the regional distribution of trends in annual maximum precipitation [71]. The most extreme event from year to year might take place at different seasons. Moderate, prolonged winter rain or snowfall might increase annual maximum precipitation on a multi-daily scale, while local, summer rain showers might dominate the results for the daily scale.

4.2 The effect of assuming non-stationarity when estimating return levels

This study's most vital insight is the higher estimated design storms when considering non-stationarity, i.e. climate change. The absolute and relative differences in highest daily annual precipitation (return levels) varied among locations and ranged between 6.7 mm/day (9%) to 27 mm/day (+48 %) for a 25-year recurrence interval (return period). Strict comparison between the stations is not possible due to varying data records. The highest absolute difference was shown in south-east Sweden, yet substantial differences were also estimated in the north, central and south-west Sweden (section 3.2).

The absolute difference in return levels for longer durations (2-day, 3-day...7-day precipitation events) show higher values for design storms estimated assuming non-stationarity. The size of the absolute difference for individual stations decreased for longer durations, expect for station 3, where the absolute difference increased. This indicates that the non-stationary assumption strongly affects the shorter durations. The difference in non-stationary return levels relative to stationary return levels decreases or varies with increasing duration, depending on station. This hints at the actual impact of non-stationarity for different durations. At station 19, for example, the difference between the non-stationary and stationary return level is higher regarding relative change for the 5-day precipitation event than for the 3-day and 7-day precipitation events, however the absolute difference is highest for the 1-day event table 3.3. Furthermore, the absolute and relative difference between return levels decreased in general for higher return periods (figure 3.13, figure 3.14, table 3.1, table 6.2), indicating a more substantial influence of non-stationarity on return levels with shorter recurrence intervals.

The uncertainty bounds for the absolute difference in non-stationary and stationary return levels decreased with increasing duration, due to decreased variability in the data records for longer durations, i.e. the data were mean values of daily precipitation. The uncertainty bounds increased for the corresponding relative differences because the influence of the estimated return levels on the ensemble was extracted. Moreover, the uncertainty bounds increased with increasing return period (figure 3.13 and figure 3.14), thereby reducing the reliability of predicted design storms for higher return periods [7].

4.3 Future climate scenarios, socio-economic aspects and the definition of non-stationarity

Future climate scenarios (RCP8,5) provided by the Swedish Meteorological and Hydrological Institute, show that the difference in annual maximum daily precipitation increases 20 to 30 % in 2071-2100 compared to 1971-2000 for all of Sweden. The annual maximum 7-day precipitation increases 15 to 30 % for the same time interval (Scenarios are found at smhi.se/klimat). This is in line with the results in section 3.2 and section 3.3, indicating that design storms assuming extreme precipitation will stay the same over time underestimate extreme events compared to estimates assuming that the extreme precipitation might increase over time.

Within hydraulic and hydrological engineering, applying appropriate design storms is crucial for designing reliable and durable construction works. The design affects societal costs and the feasibility of proposed construction work solutions [58, 47]. We show that using a stationary approach when deriving design storms potentially underestimates extreme precipitation events at some locations in Sweden. This indicates possible undersized constructions. On the other hand, the application of a non-stationary approach may overestimate design storms at sites with no indications of a future increase in extreme precipitation events. This can lead to oversized and unnecessarily expensive constructions. In Sweden, climate factors derived from future climate scenarios are commonly applied to account for climate change within construction works. This simple approach is more generalized but might increase the risk of over-sized construction works.

Another discussion topic is if, by definition, the non-stationary approach really leaves stationarity out. For example, when the distribution characteristics of the hydrological variable change with time, the mean value will be a deterministic function of time and not from random variables, thereby introducing stationarity. Montanari and Koutsoyiannis (2014) argue that changes in processes statistics, which are unpredictable or unknown, imply a stationary approach and the non-stationary description is only justified if the evolution of hydrological characteristics and parameters in time are known [47]. The parameters estimated with NEVA for the non-stationary approach (θ, β_1 and β_2; equation (2.3)) need to be given a physical explanation in terms of information about the change in the atmosphere's temperature and consequently water-vapor content. The method assumes climate change will increase precipitation linearly over time (C-C relationship) and deserves the description of being non-stationary. [47]

4.4 Model performance and Method limitations

Visual inspection of the NEVA output and the QQ-plots (section 3.2 and section 6.3) were used to investigate the model's performance. The empirical values were within the ensemble at all investigated stations, but at station 9 and 12 the empirical return levels were close to the 5th percentile of the ensemble, indicating that the model overestimates the return level. The quantiles of the annual maximum precipitation is fairly proportional to the empirical values in the QQ-plots figure 6.1, justifying the chosen parameter set up for the GEV distribution in the stationary case.

Data quantity and quality are both crucial for prediction reliability. Continuous precipitation records extending far back in time are rare and data quality varies as measurement techniques evolve. This study assumes that the SMHI data represents the precipitation well enough, although a comprehensive update to the weather stations in the 1970's might have introduced a bias into the analysis, thus affecting the results. Furthermore, difficulties and uncertainties in trend analysis are greater for extreme value analysis due to the infrequency of extreme events. 50 year long data records are a stated guideline for extreme value analysis regarding annual maximum precipitation. However, paleoclimatic records indicate that in many regions of the world the past decades do not fully represent natural climate variability. Hence, these trends found in extreme events over a 50-year period might not be caused by climate change [58].

The Mann-Kendall trend test is a non-parametric test of monotonic trends, i.e. a gradual change in relation to an independent variable (e.g. time) that is consistent in direction. The method needs long continuous records but can lack insight into a trend's causes as well as have difficulty accounting for variability caused by other climate variables, such as wind direction. For example, in southern Sweden wind effects are of special interest when analyzing precipitation due to its proximity to storm tracks. Before performing trend analysis the influence of covariate variables such as wind direction can be extracted from the data. Selecting the appropriate covariate is critical and can significantly affect the results and further analysis. The Mann-Kendall trend test does not explicitly account for step changes in observations, i.e. abrupt shifts. Including step-change analysis could provide more information about the precipitation characteristics.

NEVA is based on the assumption that precipitation intensities increase linearly with time (non-stationarity). Introducing non-stationarity increases the variability of the estimated return levels by increasing the number of parameters. However, if the assumption of non-stationarity captures the observed behavior of extreme precipitation events, the reduced bias in the estimated return levels compensates for the increased uncertainty due to more parameters [47]. The definition of non-stationarity is not designed to capture cyclical patterns of the observations. Also, the estimated return levels are based on point measurements. The local precipitation variation can be substantial, which limits the validity and hence the application area for the estimated design storms [26].

4.5 Recommendation for future studies

In Sweden, the North Atlantic Oscillation (NAO) is believed to affect precipitation in general and also the likelihood of extreme events [55]. For that reason, future research in this area should introduce the relation between NAO and annual maximum precipitation into extreme value analysis, i.e. physically based covariates [31] . Then, more representative estimates of return levels could be achievable and offer more reliable IDF-curves for infrastructure design.

To increase the spatial validity of the estimated return levels, an approach that includes the homogenization of data records could be applied. This would increase the IDF-curves' applicability, although that approach might reduce the variability of extreme precipitation events at certain locations [39, 41, 40]. Longer data records should be analyzed to test if the derived trends in extreme precipitation can be related to climate change or not, since previous studies emphasize the difficulties accounting for long term natural variability [3]. Finally, using one or two time-invariant distribution parameters could improve model performance as well as predicted return levels.

Chapter 5

Conclusions

Global warming is believed to increase and/or intensify extreme precipitation events by increasing average global temperature. In determining design storms for infrastructural design and failure risk assessment, it is commonly assumed that the statistics of extreme precipitation do not change significantly over time, a notion known as stationarity. This notion assumes that the statistics of future extreme precipitation events will be similar to those of historical observations. Therefore, the consequences of using a stationary assumption as an alternative to a non-stationary framework that does consider temporal changes in statistics of extremes was investigated. Stationary and non-stationary return levels for 10-year to 50-year extreme precipitation events for different durations (1-day, 2-day, ..., 7-day precipitation events), based on Sweden's observed daily precipitation, were evaluated. Non-stationary frequency analysis was only considered for stations with statistically significant trends over the past 50 years at 95% confidence. Non-stationary return levels were estimated using the General Extreme Value distribution with time-dependent parameters, inferred using a Bayesian approach. Finally, the estimated return levels were compared in terms of duration, recurrence interval and location.

The outcome indicates that precipitation extremes have intensified during the last 50 years and led to higher estimated return levels at 15 % of the examined locations in Sweden. The largest relative difference between the two approaches was about 40 % for the medium risk (50th percentile of parameter distribution) and up to 60 % for the low risk (95th percentile of parameter distribution). The absolute difference in estimated return levels assuming non-stationary and stationary conditions, respectively, decreases with increasing duration. This indicates that the assumption of stationarity is more severe on a daily scale. Climate factors, frequently used in Sweden for adapting infrastructure design to climate change, might contribute to underestimating and sometimes overestimating extreme events at individual locations. NEVA provides a more site-specific estimate of design storms that might give valuable information to construction projects. However, the assumption that precipitation increases linearly with time might be a serious simplification and thus reduce the model's predictability in areas such as northern Europe.[55]

The 20 stations showing an increasing trend in annual maximum precipitation over time constitute only a minor fraction of all investigated stations. This substantiates studies that have low confidence that climate change will bring intensified precipitation to Europe [58]. Moreover, the number of stations holding a trend increased up to 30 % for longer durations, a finding that supports studies showing prolonged precipitation events may cause flooding in Sweden [3]. Assuming 50 years does not overcome the natural variability in extreme precipitation events, extending the records farther back in time may remove trends and question the reliability of the predicted design storms [58].

Bibliography

[1] L. V. Alexander, X. Zhang, T. C. Peterson, J. Caesar, B. Gleason, A. M. G. Klein Tank, M. Haylock, D. Collins, B. Trewin, F. Rahimzadeh, A. Tagipour, K. Rupa Kumar, J. Revadekar, G. Griffiths, L. Vincent, D. B. Stephenson, J. Burn, E. Aguilar, M. Brunet, M. Taylor, M. New, P. Zhai, M. Rusticucci, and J. L. Vazquez-Aguirre. Global observed changes in daily climate extremes of temperature and precipitation. *Journal of Geophysical Research: Atmospheres*, 111(D5):n/a–n/a, 2006.

[2] Santosh K. Aryal, Bryson C. Bates, Edward P. Campbell, Yun Li, Mark J. Palmer, and Neil R. Viney. Characterizing and modeling temporal and spatial trends in rainfall extremes. *Journal of Hydrometeorology*, 10(1):241–253, 2015/12/25 2009.

[3] Lars Bengtsson and Arun Rana. Long-term change of daily and multi-daily precipitation in southern sweden. *Hydrological Processes*, 28(6):2897–2911, 2014.

[4] Peter Berg, Christopher Moseley, and Jan O Haerter. Strong increase in convective precipitation in response to higher temperatures. *Nature Geoscience*, 6(3):181–185, 2013.

[5] Aristita Busuioc, Deliang Chen, and Cecilia Hellström. Temporal and spatial variability of precipitation in sweden and its link with the large-scale atmospheric circulation. *Tellus A*, 53(3):348–367, 2001.

[6] Cheng-lung Chen. Rainfall intensity-duration-frequency formulas. *Journal of Hydraulic Engineering*, 109(12):1603–1621, 1983.

[7] Linyin Cheng and Amir AghaKouchak. Nonstationary precipitation intensity-duration-frequency curves for infrastructure design in a changing climate. *Scientific Reports*, 4:7093 EP –, 11 2014.

[8] Linyin Cheng, Amir AghaKouchak, Eric Gilleland, and Richard W Katz. Non-stationary extreme value analysis in a changing climate. *Climate Change*, 127(2):353–369, 2014.

[9] Daniel Cooley. Return periods and return levels under climate change. In *Extremes in a Changing Climate*, pages 97–114. Springer, 2013.

[10] L. K. Cunha, W. F. Krajewski, R. Mantilla, and L. Cunha. A framework for flood risk assessment under nonstationary conditions or in the absence of historical data. *Journal of Flood Risk Management*, 4(1):3–22, 2011.

[11] Bengt Dahlstrom. Rain intensity in sweden - a climatological analysis. Technical Report 2006-26, Swedish Meterological and Hydrological Institute, 2006 2006.

31

[12] Lisa Damberg and Amir AghaKouchak. Global trends and patterns of drought from space. 117(3-4):441–448, 2014.

[13] Seita Emori and SJ Brown. Dynamic and thermodynamic changes in mean and extreme precipitation under changed climate. *Geophysical Research Letters*, 32(17), 2005.

[14] Theodore A. Endreny and Nana Imbeah. Generating robust rainfall intensity–duration–frequency estimates with short-record satellite data. *Journal of Hydrology*, 371(1–4):182 – 191, 2009.

[15] E. Foufoula-Georgiou. A probabilistic storm transposition approach for estimating exceedance probabilities of extreme precipitation depths. *Water Resources Research*, 25(5), 1989.

[16] H. J. Fowler and C. G. Kilsby. A regional frequency analysis of united kingdom extreme rainfall from 1961 to 2000. *International Journal of Climatology*, 23(11):1313–1334, 2003.

[17] Eric Gilleland and Richard W Katz. New software to analyze how extremes change over time. *Eos, Transactions American Geophysical Union*, 92(2):13–14, 2011.

[18] B. Graler, M. J. van den Berg, S. Vandenberghe, A. Petroselli, S. Grimaldi, B. De Baets, and N. E. C. Verhoest. Multivariate return periods in hydrology: a critical and practical review focusing on synthetic design hydrograph estimation. *Hydrology and Earth System Sciences*, 17(4):1281–1296, 2013.

[19] Ida Bülow Gregersen, Henrik Madsen, Dan Rosbjerg, and Karsten Arnbjerg-Nielsen. A spatial and nonstationary model for the frequency of extreme rainfall events. *Water Resources Research*, 49(1):127–136, 2013.

[20] IdaBülow Gregersen, Henrik Madsen, Dan Rosbjerg, and Karsten Arnbjerg-Nielsen. Long term variations of extreme rainfall in denmark and southern sweden. 44(11-12):3155–3169, 2015.

[21] Salvatore Grimaldi and Francesco Serinaldi. Asymmetric copula in multivariate flood frequency analysis. *Advances in Water Resources*, 29(8):1155 – 1167, 2006.

[22] Hoshin V. Gupta, Harald Kling, Koray K. Yilmaz, and Guillermo F. Martinez. Decomposition of the mean squared error and nse performance criteria: Implications for improving hydrological modelling. *Journal of Hydrology*, 377(1–2):80–91, 10 2009.

[23] Teklu T Hailegeorgis, Donald H Burn, and P Eng. Uncertainty assessment of the impacts of climate change on extreme precipitation events. *Report prepared for the Canadian Foundation for Climate and Atmospheric Sciences project: Quantifying the uncertainty in modelled estimates of future extreme precipitation events, Department of Civil and Environmental Engineering, University of Waterloo, Waterloo, Ont., Canada*, 2009.

[24] Martin Hanel, T. Adri Buishand, and Christopher A. T. Ferro. A nonstationary index flood model for precipitation extremes in transient regional climate model simulations. *Journal of Geophysical Research: Atmospheres*, 114(D15):n/a–n/a, 2009.

[25] Zengchao Hao, Amir AghaKouchak, and Thomas J Phillips. Changes in concurrent monthly precipitation and temperature extremes. *Environmental Research Letters*, 8(3):034014, 2013.

[26] P. Harremoës and P. S. Mikkelsen. Properties of extreme point rainfall i: Results from a rain gauge system in denmark. *Atmospheric Research*, 37(4):277–286, 8 1995.

[27] E. Hassanzadeh, A. Nazemi, and A. Elshorbagy. Quantile-based downscaling of precipitation using genetic programming: Application to idf curves in saskatoon. *Journal of Hydrologic Engineering*, 19(5):943–955, 2015/12/25 2013.

[28] Dennis R Helsel and Robert M Hirsch. Statistical methods in water resources. Technical Report 04-A3, U.S. Geological Survey, 2002.

[29] Dörte Jakob. Nonstationarity in extremes and engineering design. In *Extremes in a Changing Climate*, pages 363–417. Springer, 2013.

[30] Richard W Katz. Statistics of extremes in climate change. *Climatic Change*, 100(1):71–76, 2010.

[31] Richard W Katz. Statistical methods for nonstationary extremes. In *Extremes in a Changing Climate*, pages 15–37. Springer, 2013.

[32] M.N. Khaliq, T.B.M.J. Ouarda, J.-C. Ondo, P. Gachon, and B. Bobée. Frequency analysis of a sequence of dependent and/or non-stationary hydro-meteorological observations: A review. *Journal of Hydrology*, 329(3–4):534 – 552, 2006.

[33] Kenneth E Kunkel, Thomas R Karl, David R Easterling, Kelly Redmond, John Young, Xungang Yin, and Paula Hennon. Probable maximum precipitation and climate change. *Geophysical Research Letters*, 40(7):1402–1408, 2013.

[34] V. Kveton and M. Zak. Extreme precipitation events in the czech republic in the context of climate change. *Advances in Geosciences*, 14:251–255, 2008.

[35] Jan Kyselỳ. Trends in heavy precipitation in the czech republic over 1961–2005. *International Journal of Climatology*, 29(12):1745–1758, 2009.

[36] Geert Lenderink and Erik van Meijgaard. Increase in hourly precipitation extremes beyond expectations from temperature changes. *Nature Geosci*, 1(8):511–514, 08 2008.

[37] Antonia Longobardi and Paolo Villani. Trend analysis of annual and seasonal rainfall time series in the mediterranean area. *International Journal of Climatology*, 30(10):1538–1546, 2010.

[38] Ewa B Łupikasza, Stephanie Hänsel, and Jörg Matschullat. Regional and seasonal variability of extreme precipitation trends in southern poland and central-eastern germany 1951–2006. *International Journal of Climatology*, 31(15):2249–2271, 2011.

[39] H. Madsen, P.S. Mikkelsen, D. Rosbjerg, and P. Harremoës. Estimation of regional intensity-duration-frequency curves for extreme precipitation. *Water Science and Technology*, 37(11):29 – 36, 1998. Use of Historical Rainfall Series for Hydrological ModellingSelected Proceedings of the Third International Workshop on Rainfall in Urban Areas.

[40] Henrik Madsen, Karsten Arnbjerg-Nielsen, and Peter Steen Mikkelsen. Update of regional intensity–duration–frequency curves in denmark: Tendency towards increased storm intensities. *Atmospheric Research*, 92(3):343 – 349, 2009. 7th International Workshop on Precipitation in Urban Areas7th International Workshop on Precipitation in Urban Areas.

[41] Henrik Madsen, Peter Steen Mikkelsen, Dan Rosbjerg, and Poul Harremoës. Regional estimation of rainfall intensity-duration-frequency curves using generalized least squares regression of partial duration series statistics. *Water Resources Research*, 38(11):21–1–21–11, 2002.

[42] D. Maraun, T. J. Osborn, and N. P. Gillett. United kingdom daily precipitation intensity: improved early data, error estimates and an update from 2000 to 2006. *International Journal of Climatology*, 28(6):833–842, 2008.

[43] Gerald A Meehl, Julie M Arblaster, and Claudia Tebaldi. Understanding future patterns of increased precipitation intensity in climate model simulations. *Geophysical Research Letters*, 32(18), 2005.

[44] Gerald A. Meehl, Thomas Karl, David R. Easterling, Stanley Changnon, Roger Pielke, David Changnon, Jenni Evans, Pavel Ya Groisman, Thomas R. Knutson, Kenneth E. Kunkel, Linda O. Mearns, Camille Parmesan, Roger Pulwarty, Terry Root, Richard T. Sylves, Peter Whetton, and Francis Zwiers. An introduction to trends in extreme weather and climate events: Observations, socioeconomic impacts, terrestrial ecological impacts, and model projections*. *Bulletin of the American Meteorological Society*, 81(3):413–416, 2015/11/07 2000.

[45] Seung-Ki Min, Xuebin Zhang, Francis W. Zwiers, and Gabriele C. Hegerl. Human contribution to more-intense precipitation extremes. *Nature*, 470(7334):378–381, 02 2011.

[46] Anders Moberg, Philip D Jones, David Lister, Alexander Walther, Manola Brunet, Jucundus Jacobeit, Lisa V Alexander, Paul M Della-Marta, Juerg Luterbacher, Pascal Yiou, et al. Indices for daily temperature and precipitation extremes in europe analyzed for the period 1901–2000. *Journal of Geophysical Research: Atmospheres (1984–2012)*, 111(D22), 2006.

[47] Alberto Montanari and Demetris Koutsoyiannis. Modeling and mitigating natural hazards: Stationarity is immortal! *Water Resources Research*, 50(12):9748–9756, 2014.

[48] Victor Ntegeka and Patrick Willems. Trends and multidecadal oscillations in rainfall extremes, based on a more than 100-year time series of 10 min rainfall intensities at uccle, belgium. *Water Resources Research*, 44(7), 2008.

[49] Timothy J. Osborn and Mike Hulme. Evidence for trends in heavy rainfall events over the uk. *Philosophical Transactions of the Royal Society of London A: Mathematical, Physical and Engineering Sciences*, 360(1796):1313–1325, 2002.

[50] Jouni Räisänen and Rune Joelsson. Changes in average and extreme precipitation in two regional climate model experiments. *Tellus A*, 53(5):547–566, 2001.

[51] Benjamin Renard, Michel Lang, and Philippe Bois. Statistical analysis of extreme events in a non-stationary context via a bayesian framework: case study with peak-over-threshold data. 21(2):97–112, 2006.

[52] John C Rodda, Max A Little, Harvey JE Rodda, and Patrick E McSharry. A comparative study of the magnitude, frequency and distribution of intense rainfall in the united kingdom. *International Journal of Climatology*, 30(12):1776–1783, 2010.

[53] J. Salas and J. Obeysekera. Revisiting the concepts of return period and risk for non-stationary hydrologic extreme events. *Journal of Hydrologic Engineering*, 19(3):554–568, 2015/12/25 2013.

[54] G. Salvadori and C. De Michele. Multivariate multiparameter extreme value models and return periods: A copula approach. *Water Resources Research*, 46(10), 2010.

[55] Adam A Scaife, Chris K Folland, Lisa V Alexander, Anders Moberg, and Jeff R Knight. European climate extremes and the north atlantic oscillation. *Journal of Climate*, 21(1):72–83, 2008.

[56] O Seidou, TBMJ Ouarda, M Barbet, P Bruneau, and B Bobee. A parametric bayesian combination of local and regional information in flood frequency analysis. *Water Resources Research*, 42(11), 2006.

[57] Tido Semmler and Daniela Jacob. Modeling extreme precipitation events—a climate change simulation for europe. *Global and Planetary Change*, 44(1–4):119 – 127, 2004. Extreme climatic events.

[58] N. Nicholls D. Easterling C.M. Goodess S. Kanae J. Kossin Y. Luo J. Marengo K. McInnes M. Rahimi M. Reichstein A. Sorteberg C. Vera Seneviratne, S.I. and X. Zhang. Changes in climate extremes and their impacts on the natural physical environment. in: Managing the risks of extreme events and disasters to advance climate change adaptation [field, c.b., v. barros, t.f. stocker, d. qin, d.j. dokken, k.l. ebi, m.d. mastrandrea, k.j. mach, g.-k. plattner, s.k. allen, m. tignor, and p.m. midgley (eds.)]. *A Special Report of Working Groups I and II of the Intergovernmental Panel on Climate Change (IPCC)*, pages 109–230, 2012.

[59] S.P. Simonovic and A. Peck. Updated rainfall intensity duration frequency curves for the city of london under the changing climate. Technical report, The University of Western Onatario, 2009.

[60] Thomas Skaugen, Marit Astrup, Lars A. Roald, and Eirik Førland. Scenarios of extreme daily precipitation for norway under climate change. *Hydrology Research*, 35(1):1–13, 2004.

[61] T.F. Stocker, D. Qin, G.-K. Plattner, M. Tignor, S.K. Allen, J. Boschung, A. Nauels, Y. Xia, V. Bex, and P.M. Midgley. *Climate Change 2013: The physical science basis: Working group I contribution to the fifth assessment report of the Intergovernmental Panel on Climate Change*. Cambridge University Press, Cambride, United Kingdom and New York, NY, USA 1535 pp., 2013.

[62] W.G. Strupczewski, V.P. Singh, and W. Feluch. Non-stationary approach to at-site flood frequency modelling i. maximum likelihood estimation. *Journal of Hydrology*, 248(1–4):123 – 142, 2001.

[63] Shigetoshi Sugahara, Rosmeri Porfírio da Rocha, and Reinaldo Silveira. Non-stationary frequency analysis of extreme daily rainfall in sao paulo, brazil. *International Journal of Climatology*, 29(9):1339–1349, 2009.

[64] Kevin E Trenberth. Changes in precipitation with climate change. *Climate Research*, 47(1):123, 2011.

[65] Kevin E Trenberth. Changes in precipitation with climate change. *Climate Research*, 47(1):123, 2011.

[66] S Trömel and C-D Schönwiese. Probability change of extreme precipitation observed from 1901 to 2000 in germany. *Theoretical and Applied Climatology*, 87(1-4):29–39, 2007.

[67] Seth Westra, Lisa V Alexander, and Francis W Zwiers. Global increasing trends in annual maximum daily precipitation. *Journal of Climate*, 26(11):3904–3918, 2013.

[68] P. Willems. Adjustment of extreme rainfall statistics accounting for multidecadal climate oscillations. *Journal of Hydrology*, 490:126 – 133, 2013.

[69] A. Yilmaz and B. Perera. Extreme rainfall nonstationarity investigation and intensity–frequency–duration relationship. *Journal of Hydrologic Engineering*, 19(6):1160–1172, 2015/12/25 2013.

[70] Xuebin Zhang, Jiafeng Wang, Francis W. Zwiers, and Pavel Ya Groisman. The influence of large-scale climate variability on winter maximum daily precipitation over north america. *Journal of Climate*, 23(11):2902–2915, 2015/12/25 2010.

[71] Feifei Zheng, Seth Westra, and Michael Leonard. Opposing local precipitation extremes. *Nature Clim. Change*, 5(5):389–390, 05 2015.

[72] Jianting Zhu, Mark C. Stone, and William Forsee. Analysis of potential impacts of climate change on intensity–duration–frequency (idf) relationships for six regions in the united states. *Journal of Water and Climate Change*, 3(3):185–196, 2012.

Chapter 6

Appendix

6.1 P-values for trends in annual maximum precipitation

Table 6.1: Significance level (p-value) for all stations showing a significant trend in daily annual maximum precipitation. Significance levels for 2, 3, 4, 5, 6, 7 days are also presented. Twelve stations held a significant trend through all durations, namely stations 3, 4, 7, 8, 9, 11, 12, 14, 16, 17, 19 and 20.

Station	1-day	2-day	3-day	4-day	5-day	6-day	7-day
1	**0.01**	0.02	0.04	0.23	0.16	0.13	0.019
2	**0.004**	0.14	0.12	0.21	0.16	0.18	0.32
3	**0.03**	0.03	3.54 E-3	1.7 E-3	2.4 E-3	9.8 E-4	1.6 E-3
4	**0.03**	0.006	0.02	2.5 E-3	7.6 E-3	6.7 E-3	9.7 E-3
5	**0.02**	0.02	4.5E-2	0.20	0.20	0.13	0.20
6	**0.02**	0.01	0.01	0.06	0.09	0.04	0.04
7	**0.01**	0.02	0.02	3.6 E-3	6.1 E-3	2.1 E-3	1.1 E-3
8	**1.3 E-3**	3.0 E-5	2.7E-3	1.9 E-3	3.6 E-3	0.01	0.02
9	**0.02**	5.3E-3	0.02	0.02	0.01	0.01	0.01
10	**0.02**	0.005	2.3 E-3	0.02	0.03	0.08	0.12
11	**3.3 E-3**	1.6E-3	0.02	9.3 E-2	6.7 E-3	7.7 E-3	6.7 E-3
12	**0.05**	0.02	1.3 E-3	2.9 E-3	4.7 E-3	3.4 E-3	3.6 E-3
13	**0.02**	0.06	0.31	0.15	0.19	0.14	0.33
14	**0.005**	0.045	0.01	6.1 E-3	2.5 E-3	1.3 E-3	1.5 E-3
15	**0.04**	0.03	0.01	0.11	0.14	0.08	0.02
16	**6.3E-3**	3.0 E-5	1 E-5	1.0 E-4	1.0 E-4	4.0 E-4	8.0 E-4
17	**0.047**	6.4 E-3	4.5 E-4	2.9 E-3	1.1 E-2	1.6 E-3	1.0 E-3
18	**0.01**	0.03	0.07	0.01	0.01	0.04	0.04
19	**0.01**	0.01	0.02	4.5 E-3	9.1 E-3	7.4 E-3	2.4 E-3
20	**0.01**	0.003	6.8 E-3	0.01	0.01	0.01184	5.4 E-3
21	**0.02**	0.01	0.02	0.01	0.00664	3.01 E-3	5.0 E-3

6.2 Differences in non-stationary and stationary return levels

Table 6.2: Medium risk; The absolute difference between the highest annual daily precipitation (return level; mm/day) for 10- and 50-years return periods, estimated assuming non-stationary and stationary conditions, respectively, for the 20 stations with increasing trends. The medians (p_{50}) are boldfaced, representing the estimated return levels, while the 5th and 95th percentile (p_5 and p_{95}) constitute uncertainty bounds.

T	10 years			50 years		
Station	p_5	p_{50}	p_{95}	p_5	p_{50}	p_{95}
1	-10.0	**5.5**	19.4	-53.7	**7.0**	54.2
2	5.9	**17.6**	29.0	-2.2	**15.1**	30.4
3	-8.7	**3.2**	13.0	-29.4	**2.1**	23.7
4	1.2	**10.9**	18.2	-7.6	**10.9**	22.6
5	6.9	**12.7**	17.6	3.8	**13.4**	19.7
6	-4.7	**11.9**	25.4	-32.1	**8.8**	34.2
7	-8.4	**5.9**	19.7	-25.6	**0.1**	19.2
8	18.4	**27.8**	35.5	12.0	**26.0**	34.6
9	-3.9	**11.9**	24.7	-35.9	**-1.6**	26.2
10	6.2	**14.3**	22.0	2.3	**14.3**	25.6
11	-1.3	**7.8**	16.1	-20.1	**7.2**	24.6
12	-0.7	**15.2**	29.1	-39.1	**2.0**	29.0
14	8.2	**25.4**	42.5	-7.5	**21.2**	46.8
15	7.5	**18.0**	29.1	0.1	**21.6**	33.8
16	-1.0	**11.8**	23.3	-46.5	**8.9**	43.7
17	3.2	**17.1**	29.4	-6.5	**17.3**	39.4
18	4.9	**17.9**	32.0	-15.1	**12.4**	30.4
19	-1.8	**6.3**	13.6	-17.9	**4.9**	21.9
20	-0.5	**8.2**	16.7	-13.7	**7.3**	26.1
21	-3.0	**4.0**	10.6	-3.0	**9.2**	26.0

Table 6.3: Low risk; The absolute difference between the highest annual multi-daily precipitation(return level; mm/day) for 10- and 50-year return periods estimated assuming non-stationary and stationary conditions, respectively. The return levels are estimated for the 12 stations with trends for 1, 2, 3, 4, 5, 6, 7 days. The medians (p_{50}) are boldfaced, representing the estimated return level, while the 5th and 95th percentile (p_5 and p_{95}) constitute uncertainty bounds.

| T | 10 yr | | | 50 yr | | |
Station	p_5	p_{50}	p_{95}	p_5	p_{50}	p_{95}
3	-2.7	**3.7**	10.4	-1.3	**4.0**	8.8
4	0.4	**12.0**	21.9	-1.7	**8.0**	14.1
7	1.3	**8.4**	14.9	-2.1	**3.0**	8.5
8	4.5	**10.5**	17.5	3.9	**8.4**	12.5
9	0.1	**7.6**	17.2	8.6	**13.5**	19.3
11	-1.9	**5.9**	13.9	-1.5	**3.0**	7.6
12	-3.3	**6.6**	12.8	-0.1	**5.5**	10.3
14	4.4	**13.0**	22.5	8.2	**13.2**	19.2
16	-6.1	**7.8**	15.0	-3.3	**4.6**	12.4
17	4.4	**14.3**	23.9	3.1	**11.5**	17.9
19	-0.0	**6.7**	12.5	1.8	**5.6**	10.0
20	9.1	**14.7**	22.4	4.8	**7.7**	10.6

Table 6.4: Low risk; The relative difference between the highest annual multi-daily precipitation(return level; %) for 10- and 50-year return periods, estimated assuming non-stationary and stationary conditions respectively. The return levels are estimated for the 12 stations with trends for 1, 2, 3, 4, 5, 6, 7 days. The medians (p_{50}) are boldfaced, representing the estimated return level, while the 5th and 95th percentile (p_5 and p_{95}) constitute uncertainty bounds.

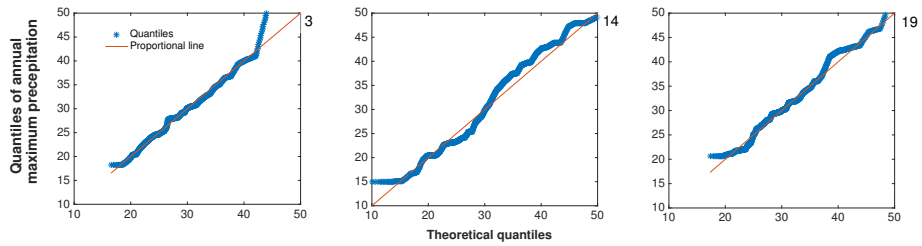| T | 10 yr | | | 50 yr | | |
Station	p_5	p_{50}	p_{95}	p_5	p_{50}	p_{95}
3	-8.9	**14.2**	44.4	-6.5	**21.9**	49.8
4	1.2	**43.9**	88.2	-6.5	**41.3**	77.3
7	4.3	**30.5**	58.1	-9.7	**15.9**	45.6
8	15.3	**38.4**	66.2	18.9	**41.9**	63.7
9	0.2	**25.2**	61.2	38.5	**64.1**	97.7
11	-6.4	**22.2**	56.2	-7.6	**16.5**	42.9
12	-8.9	**24.1**	51.6	-0.4	**29.5**	57.8
14	13.8	**45.7**	83.3	39.7	**71.0**	108.2
16	-14.2	**24.3**	54.7	-12.5	**21.0**	63.7
17	12.7	**47.9**	85.1	12.9	**51.6**	87.2
19	-0.0	**26.1**	51.3	9.2	**31.0**	58.4
20	35.6	**58.4**	91.6	25.6	**42.4**	59.7

6.3 Model performance

Figure 6.1: Quantiles for daily annual maximum precipitation versus quantiles of the General Extreme Value distribution for stations 3, 14 and 19 (QQ-plot). The data fits the particular GEV distributions fairly well, except at the high end of the range.
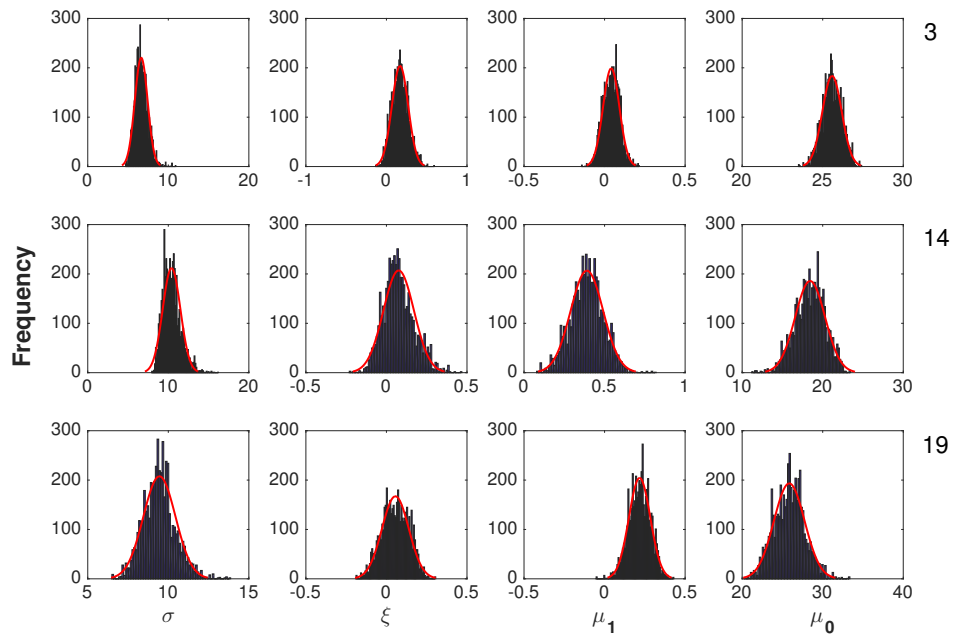

Figure 6.2: The distributions of the General Extreme Value (GEV) distribution parameters, $\beta_1 = (\mu_1, \mu_0, \sigma, \xi)$ for stations 3, 14 and 19, assuming non-stationary conditions. The distributions are compared with the normal distribution to investigate convergence to one final GEV, from which the return levels for different return periods can be found(equation (2.2) and equation (2.3)).